LOCAL DISCONTINUOUS GALERKIN SCHEMES FOR A NONLINEAR VARIATIONAL WAVE EQUATION MODELING LIQUID CRYSTALS

P. AURSAND AND U. KOLEY

Abstract. We consider a nonlinear variational wave equation that models the dynamics of nematic liquid crystals. Discontinuous Galerkin schemes that either conserve or dissipate a discrete version of the energy associated with these equations are designed. Numerical experiments illustrating the stability and efficiency of the schemes are presented. An interesting feature of these schemes is their ability to approximate two distinct weak solutions of the underlying system.

1. Introduction

1.1. **The model.** The dynamics of liquid crystals is of utmost significance to the makers of visual displays such as LCDs. Liquid crystals are mesophases, i.e. intermediate states of matter between the liquid and the crystal phase. They exhibit characteristics of fluid flow and have optical properties typically associated with crystals. One of the most common phases in liquid crystals is the nematic phase. Nematic liquid crystals consist of strongly elongated molecules that can be considered invariant under rotation by an angle of π. The flow of a liquid crystal is commonly described by two linearly independent vector fields; one describing the fluid flow and one describing the orientation of the so-called director field that gives the orientation of the rod-like molecule. In this paper we will only consider stationary flow, and hence focus exclusively on the dynamics of the director field

$$\mathbf{n} = \mathbf{n}(\mathbf{x}, t) \in \mathcal{S}^2.$$

Given a director field $\mathbf{n}$, the well known Oseen-Frank free-energy density $\mathbf{W}$ associated with this field is given by

$$\mathbf{W}(\mathbf{n}, \nabla\mathbf{n}) = \alpha \left|\mathbf{n} \times (\nabla \times \mathbf{n})\right|^2 + \beta \left(\nabla \cdot \mathbf{n}\right)^2 + \gamma \left(\mathbf{n} \cdot (\nabla \times \mathbf{n})\right)^2. \tag{1.1}$$

The positive constants α, β and γ are elastic constants of the liquid crystal. Note that each term on the right hand side of (1.1) arises from different types of distortions. In particular, the term $\alpha \left|\mathbf{n} \times (\nabla \times \mathbf{n})\right|^2$ corresponds to the bending of the medium, the term $\beta \left(\nabla \cdot \mathbf{n}\right)^2$ corresponds to splay, and the term $\gamma \left(\mathbf{n} \cdot (\nabla \times \mathbf{n})\right)^2$ corresponds to the twisting of the medium.

For the special case of $\alpha = \beta = \gamma$, the free-energy density (1.1) reduces to

$$\mathbf{W}(\mathbf{n}, \nabla\mathbf{n}) = \alpha \left|\nabla\mathbf{n}\right|^2,$$

which corresponds to the potential energy density used in harmonic maps into the sphere $\mathcal{S}^2$. The constrained elliptic system of equations for $\mathbf{n}$, derived from the potential (1.1) using a variational principle, and the parabolic flow associated with it, are widely studied, see [6, 11, 13] and references therein.

In the regime where inertial effects are dominating over viscosity, it is natural to model the propagation of orientation waves in the director field by employing the principle of least action [26], i.e.

$$\frac{\delta}{\delta \mathbf{n}} \iint \left(\mathbf{n}_t^2 - \mathbf{W}(\mathbf{n}, \nabla\mathbf{n})\right) dx\, dt = 0, \qquad \mathbf{n} \cdot \mathbf{n} = 1. \tag{1.2}$$

Date: September 12, 2014.

Again, in the special case of $\alpha = \beta = \gamma$, this variational principle (1.2) yields the equation for harmonic wave maps from $(1+3)$-dimensional Minkowski space into the two sphere, see [9, 27, 28] and references therein.

In this paper, we will restrict ourselves to one-dimensional planar waves; the director field $\mathbf{n}$ is given by

$$\mathbf{n}(x,t) = \cos\psi(x,t)\mathbf{e}_x + \sin\psi(x,t)\mathbf{e}_y,$$

where $\mathbf{e}_x$ and $\mathbf{e}_y$ are the coordinate vectors in the x and y directions, respectively. That is to say the dynamics of the liquid crystal is described by some unknown function ψ, which represents the angle of the director field relative to the x-direction. In this case, the variational principle (1.2) reduces to [26, 21, 16]

$$\begin{cases} \psi_{tt} - c(\psi)\left(c(\psi)\psi_x\right)_x = 0, & (x,t) \in \Pi_T, \\ \psi(x,0) = \psi_0(x), & x \in \mathbb{R}, \\ \psi_t(x,0) = \psi_1(x), & x \in \mathbb{R}, \end{cases} \tag{1.3}$$

where $\Pi_T = \mathbb{R} \times [0,T]$ with fixed $T > 0$, and the wave speed $c(\psi)$ given by

$$c^2(\psi) = \alpha\cos^2\psi + \beta\sin^2\psi. \tag{1.4}$$

The form (1.3) is the standard form of the nonlinear variational wave equation considered in the literature.

For the one-dimensional planar waves the energy is given by

$$\mathcal{E}(t) = \int_{\mathbb{R}} \left(\psi_t^2 + c^2(\psi)\psi_x^2\right)\, dx. \tag{1.5}$$

A simple calculation shows that smooth solutions of the variational wave equation (1.3) satisfy

$$\frac{d\mathcal{E}(t)}{dt} = 0. \tag{1.6}$$

1.2. **Mathematical difficulties.** Despite its apparent simplicity, the mathematical analysis of (1.3) is complicated. Independently of the smoothness of the initial data, due to the nonlinear nature of the equation, singularities may form in the solution ψ_x. Therefore, we consider solutions in the weak sense:

Definition 1.1. *Set $\Pi_T = \mathbb{R} \times (0,T)$. A function*

$$\psi(t,x) \in L^\infty\left([0,T]; W^{1,p}(\mathbb{R})\right) \cap C(\Pi_T), \psi_t \in L^\infty\left([0,T]; L^p(\mathbb{R})\right),$$

for all $p \in [1, 3+q]$, where q is some positive constant, is a weak solution of the initial value problem (1.3) *if it satisfies:*

***D**.1 For all test functions $\varphi \in \mathcal{D}(\mathbb{R} \times [0,T))$*

$$\iint_{\Pi_T} \left(\psi_t\varphi_t - c^2(\psi)\psi_x\varphi_x - c(\psi)c'(\psi)(\psi_x)^2\varphi\right)\, dx\, dt = 0. \tag{1.7}$$

***D**.2 $\psi(\cdot,t) \to u_0$ in $C\left([0,T]; L^2(\mathbb{R})\right)$ as $t \to 0^+$.*

***D**.3 $\psi_t(\cdot,t) \to v_0$ as a distribution in Π_T when $t \to 0^+$.*

An important aspect of the variational wave equation is that there exist both *conservative* and *dissipative* weak solutions, see e.g. [30] for a more detailed discussion. To illustrate this difference, one can consider initial data for which the solution vanishes identically at some specific (finite) time. At this point, at least two possibilities exist: to continue with the trivial zero solution, termed as the dissipative solution. Alternatively, one can show that there exists a nontrivial solution that appears as a natural continuation of the solution prior to the critical time. This solution is denoted the conservative solution as it preserves the total energy (1.5) of the system. This dichotomy makes the question of well-posedness of the initial value problem (1.3) very difficult. Additional admissibility conditions are needed to select a physically relevant solution. The specification of such admissibility criteria is still open.

Although the problem of global existence and uniqueness of solutions to the Cauchy problem of the nonlinear variational wave equation (1.3) is still open, several recent papers have explored related questions or particular cases of (1.3). It has been demonstrated in [17] that (1.3) is rich in structural phenomena associated with weak solutions. In fact, by rewriting the highest derivatives of (1.3) in conservative form

$$\psi_{tt} - \left(c^2(\psi)\psi_x\right)_x = -c(\psi)c'(\psi)\psi_x^2,$$

we see that the strong precompactness in L^2 of the derivatives $\{\psi_x\}$ of a sequence of approximate solutions is essential in establishing the existence of a global weak solution. However, the equation shows the phenomenon of persistence of oscillations [12] and annihilation in which a sequence of exact solutions with bounded energy can oscillate forever so that the sequence $\{\psi_x\}$ is not precompact in L^2. Still, the weak limit of the sequence is a weak solution.

There has been a number of papers concerning the existence of weak solutions of the Cauchy problem (1.3), starting with the papers by Zhang and Zheng [30, 31, 32, 33, 34, 35], Bressan and Zheng [7] and Holden and Raynaud [19]. In [34], the authors show existence of a global weak solution using the method of Young measures for initial data $\psi_0 \in H^1(\mathbb{R})$ and $\psi_1 \in L^2(\mathbb{R})$. The function $c(\psi)$ is assumed to be smooth, bounded, positive with derivative that is non-negative and strictly positive on the initial data ψ_0. This means that the analysis in [30, 31, 32, 33, 34, 35] does not directly apply to (1.3) when using the physical wave speed (1.4).

A different approach to the study of (1.3) was taken by Bressan and Zheng [7]. Here, they rewrote the equation in new variables such that the singularities disappeared. They show that for ψ_0 absolutely continuous with $(\psi_0)_x, \psi_1 \in L^2(\mathbb{R})$, the Cauchy problem (1.3) allows a global weak solution with the following properties: the solution ψ is locally Lipschitz continuous and the map $t \to u(t,\cdot)$ is continuously differentiable with values in $L^p_{\text{loc}}(\mathbb{R})$ for $1 \le p < 2$.

In [19], Holden and Raynaud prove the existence of a global semigroup for conservative solutions of (1.3), allowing for concentration of energy density on sets of zero measure. Furthermore they also allow for initial data ψ_0, ψ_1 that contain measures. The proof involves constructing the solution by introducing new variables related to the characteristics, leading to a characterization of singularities in the energy density. They also prove that energy can only focus on a set of times of zero measure or at points where $c'(\psi)$ vanishes.

1.3. **Numerical Schemes.** There are no elementary and explicit solutions available for (1.3), except for the trivial case where c is constant. Consequently, robust numerical schemes for approximating the variational wave equation are very important in the study of nematic liquid crystals. However, there is a paucity of efficient numerical schemes for these equations. Also, traditional finite difference schemes will not yield conservative solutions, but rather dissipative solutions due to the intrinsic numerical diffusion in these methods.

Within the existing literature we can refer to [16], where the authors present some numerical examples to illustrate their theory. In recent years, a semi-discrete finite difference scheme for approximating one-dimensional equation (1.3) was considered in [20]. The authors were even able to prove convergence of the numerical approximation, generated by their scheme, to the *dissipative* solution of (1.3). However, the underlying assumptions on the wave speed c (positivity of the derivative of c) precludes consideration of realistic wave speeds given by (1.4). Another recent paper dealing with numerical approximation of (1.3) is [19]. Here, the authors use their analytical construction to define a numerical method that can approximate the *conservative* solution. However, the method is computationally very expensive as there is no time marching. Another recent paper [22] deals with *first order* finite different schemes based on either the conservation or the dissipation of the energy associated with (1.3). In the one-dimensional case, they rewrote the variational wave equation (1.3) in the form of two equivalent first-order systems. Energy conservative as well as energy dissipative schemes approximating both these formulations were derived. Moreover, they also designed an energy conservative scheme based on a Hamiltonian formulation of the variational wave equation.

Furthermore, there are some works on the Ericksen–Leslie (EL) equations [1], a simple set of equations describing the motion of a nematic liquid crystal. In [5], authors have presented a finite

element scheme for the EL equations. Their approximations are based on the ideas given in [3] which utilize the Galerkin method with Lagrange finite elements of order 1. Convergence, even convergence to measure-valued solutions, of such schemes is an open problem. In [2], a saddle-point formulation was used to construct finite element approximate solutions to the EL equations.

A penalty method based on well-known penalty formulation for EL equations has been introduced in [23] which uses the *Ginzburg–Landau* function. Convergence of such approximate solutions, based on an energy method and a compactness result, towards measure valued solutions has been proved in [24].

1.4. **Scope and outline of the paper.** In view of the above discussion, there seem to exist no robust and efficient high-order numerical schemes currently available for solving the nonlinear variational wave equation (1.3). Furthermore, one can expect *conservative* as well as *dissipative* solutions of the variational wave equation (1.3) after singularity formation. Hence, there is a need for higher-order schemes (energy conservative and energy dissipative) that approximate these different types of solutions. Typically, energy conservative schemes produce oscillations at shocks. This is expected as energy needs to be dissipated at shocks. A suitable numerical diffusion operator added to energy conservative scheme results in a energy stable scheme. To the best of our knowledge, this is the first attempt to construct high-order conservative and dissipative schemes for (1.3).

We will require our numerical methods to be shock capturing, exhibit high-order accuracy and low numerical dissipation away from shocks. Shock capturing Runge-Kutta Discontinuous Galerkin methods are high-order accurate away from discontinuities, thus they are a candidate method for carrying out such simulations. Discontinuous Galerkin (DG) methods were first introduced by Hill and Reed [18] for the neutron transport equations (linear hyperbolic equations). These methods were then generalized for systems of hyperbolic conservation laws by Cockburn and co-workers [10] and references therein. In space the solution is approximated using piecewise polynomials on each element. Exact or approximate Riemann solvers from finite volume methods are used to compute the numerical fluxes between elements. Limiters or shock capturing operators are used to achieve non-oscillatory approximate solutions, if they contain shocks [8]. For these reasons, DG methods can be seen as generalization of finite volume methods to higher order.

Given this background, we present a class of schemes in this paper that has following properties:

(1) All the schemes are (formally) high-order accurate.
(2) All the designed schemes resolved the solution (including possible singularities in the angle ψ) in a stable manner.
(3) The energy conservative schemes converge to a limit solution (as the mesh is refined), whose energy is preserved. This solution is a *conservative* solution of (1.3).
(4) The energy dissipative schemes also converge to a limit solution with energy being dissipated with time. This solution is a *dissipative* solution of the variational wave equation.

The rest of the paper is organized as follows: In Section 2, we present energy conservative and energy dissipative schemes for the one-dimensional equation (1.3). Details of implementation presented in Section 3 and finally numerical experiments illustrating all these designed schemes are presented in Section 4.

2. Numerical schemes for the variational wave equation

2.1. **The grid and notation.** We begin by introducing some notation needed to define the DG schemes. Let the domain $\Omega \subset \mathbb{R}$ be decomposed as $\Omega = \cup_j \Omega_j$ where $\Omega_j = [x_{j-1/2}, x_{j+1/2}]$ for $j = 1, \cdots, N$. We denote $\Delta x_j = x_{j+1/2} - x_{j-1/2}$ and $x_j = (x_{j-1/2} + x_{j+1/2})/2$.

Let u be a grid function and denote $u^+_{j+1/2}$ as the function evaluated at the right side of the cell interface at $x_{j+1/2}$ and let $u^-_{j+1/2}$ denote the value at the left side. We can then introduce the jump, and respectively, the average of any grid function u across the interface as

$$\overline{u}_{j+1/2} := \frac{u^+_{j+1/2} + u^-_{j+1/2}}{2},$$

$$[\![u]\!]_{j+1/2} := u^+_{j+1/2} - u^-_{j+1/2}.$$

Now let v be another grid function. The following identity is readily verified:

$$[\![uv]\!]_{j+1/2} = \overline{u}_{j+1/2}[\![v]\!]_{j+1/2} + [\![u]\!]_{j+1/2}\overline{v}_{j+1/2} \tag{2.1}$$

2.2. **A first-order system of Riemann invariants.** It is easy to check that the variational wave equation (1.3) can be rewritten as a first-order system by introducing the Riemann invariants:

$$R := \psi_t + c(\psi)\psi_x$$
$$S := \psi_t - c(\psi)\psi_x$$

For smooth solutions, equation (1.3) is equivalent to the following system in non-conservative form for (R, S, ψ):

$$\begin{cases} R_t - c(\psi)R_x = \frac{c'(\psi)}{4c(\psi)}\left(R^2 - S^2\right) \\ S_t + c(\psi)S_x = -\frac{c'(\psi)}{4c(\psi)}\left(R^2 - S^2\right) \\ \psi_t = \frac{R+S}{2} \end{cases} \tag{2.2}$$

Observe that one can also rewrite the equation (1.3) in conservative form for (R, S, ψ) as

$$\begin{cases} R_t - (c(\psi)R)_x = -\frac{c_x(\psi)}{2}\left(R - S\right), \\ S_t + (c(\psi)S)_x = -\frac{c_x(\psi)}{2}\left(R - S\right), \\ \psi_t = \frac{R+S}{2}. \end{cases} \tag{2.3}$$

The corresponding energy associated with the system (2.2) is

$$\mathcal{E}(t) = \frac{1}{2}\int_{\mathbb{R}} \left(R^2 + S^2\right)\, dx. \tag{2.4}$$

A simple calculation shows that smooth solutions of (2.2) satisfy the energy identity:

$$(R^2 + S^2)_t - \left(c(\psi)(R^2 - S^2)\right)_x = 0. \tag{2.5}$$

Hence, the fact that the total energy (2.4) is conserved follows from integrating the above identity in space and assuming that the functions R, S decay at infinity.

2.3. **Variational formulation.** We seek an approximation (R, S, ψ) of (2.3) such that for each $t \in [0, T]$, R, S, and ψ belong to finite dimensional space

$$X^p_{\Delta x}(\Omega) = \left\{u \in L^2(\Omega) : u|_{\Omega_j} \text{ polynomial of degree} \le p\right\}.$$

The variational form is derived by multiplying the strong form (2.3) with test functions $\phi, \eta, \zeta \in X^p_{\Delta x}(\Omega)$ and integrating over each element separately. After integrating by parts we obtain

(2.6)

$$\begin{aligned} &\sum_{j=1}^N \int_{\Omega_j} R_t\, \phi \mathrm{d}x + \sum_{j=1}^N \int_{\Omega_j} cR\phi_x \,\mathrm{d}x - \sum_{j=1}^N (cR)(\psi(x_{j+1/2}, t))\phi^-_{j+1/2} + \sum_{j=1}^N (cR)(\psi(x_{j-1/2}, t))\phi^+_{j-1/2} \\ &= \frac{1}{2}\sum_{j=1}^N \int_{\Omega_j} c(R\phi)_x \,\mathrm{d}x - \frac{1}{2}\sum_{j=1}^N c(\psi(x_{j+1/2}, t))R^-_{j+1/2}\phi^-_{j+1/2} + \frac{1}{2}\sum_{j=1}^N c(\psi(x_{j-1/2}, t))R^+_{j-1/2}\phi^+_{j-1/2} \\ &- \frac{1}{2}\sum_{j=1}^N \int_{\Omega_j} c(S\phi)_x \,\mathrm{d}x + \frac{1}{2}\sum_{j=1}^N c(\psi(x_{j+1/2}, t))S^-_{j+1/2}\phi^-_{j+1/2} - \frac{1}{2}\sum_{j=1}^N c(\psi(x_{j-1/2}, t))S^+_{j-1/2}\phi^+_{j-1/2}, \end{aligned}$$

(2.7)

$$\begin{aligned} &\sum_{j=1}^N \int_{\Omega_j} S_t\, \eta \mathrm{d}x - \sum_{j=1}^N \int_{\Omega_j} cS\eta_x \,\mathrm{d}x + \sum_{j=1}^N (cS)(\psi(x_{j+1/2}, t))\eta^-_{j+1/2} - \sum_{j=1}^N (cS)(\psi(x_{j-1/2}, t))\eta^+_{j-1/2} \\ &= \frac{1}{2}\sum_{j=1}^N \int_{\Omega_j} c(R\eta)_x \,\mathrm{d}x - \frac{1}{2}\sum_{j=1}^N c(\psi(x_{j+1/2}, t))R^-_{j+1/2}\eta^-_{j+1/2} + \frac{1}{2}\sum_{j=1}^N c(\psi(x_{j-1/2}, t))R^+_{j-1/2}\eta^+_{j-1/2} \end{aligned}$$

$$-\frac{1}{2}\sum_{j=1}^{N}\int_{\Omega_j} c(S\eta)_x\,\mathrm{d}x+\frac{1}{2}\sum_{j=1}^{N} c(\psi(x_{j+1/2},t))S^-_{j+1/2}\eta^-_{j+1/2}-\frac{1}{2}\sum_{j=1}^{N} c(\psi(x_{j-1/2},t))S^+_{j-1/2}\eta^+_{j-1/2}$$

and

$$\sum_{j=1}^{N}\int_{\Omega_j}\psi_t\,\zeta\mathrm{d}x=\sum_{j=1}^{N}\int_{\Omega_j}\frac{R+S}{2}\,\zeta\,\mathrm{d}x. \tag{2.8}$$

To obtain a numerical scheme, the numerical fluxes $(cR)(\psi(x_{j\pm1/2},t))$, $(cS)(\psi(x_{j\pm1/2},t))$ and $(c)(\psi(x_{j\pm1/2},t))$ all need to be determined.

2.4. **Energy Preserving Scheme Based On System of Riemann Invariants.** Our objective is to design a (semi-discrete) DG scheme such that the numerical approximations conserve a discrete version of the energy (2.26). To this end, we suggest the following:

For a conservative scheme, we use the numerical flux

$$(c)(\psi(x_{j\pm1/2},t))=\overline{c}_{j\pm1/2}\quad\text{and}\quad(cf)(\psi(x_{j\pm1/2},t))=\overline{c}_{j\pm1/2}\overline{f}_{j\pm1/2}.$$

Thus, for the RS-formulation the DG scheme then becomes: Find $R,S,\psi\in X^p_{\Delta x}(\Omega)$ such that

$$\begin{aligned}
&\sum_{j=1}^{N}\int_{\Omega_j} R_t\phi\mathrm{d}x+\sum_{j=1}^{N}\int_{\Omega_j} cR\phi_x\mathrm{d}x-\sum_{j=1}^{N}\overline{c}_{j+1/2}\overline{R}_{j+1/2}\phi^-_{j+1/2}+\sum_{j=1}^{N}\overline{c}_{j-1/2}\overline{R}_{j-1/2}\phi^+_{j-1/2}\\
&\qquad=\frac{1}{2}\sum_{j=1}^{N}\int_{\Omega_j} c\,(R\phi)_x\,\mathrm{d}x-\frac{1}{2}\sum_{j=1}^{N}\overline{c}_{j+1/2}R^-_{j+1/2}\phi^-_{j+1/2}\\
&\qquad\quad+\frac{1}{2}\sum_{j=1}^{N}\overline{c}_{j-1/2}R^+_{j-1/2}\phi^+_{j-1/2}-\frac{1}{2}\sum_{j=1}^{N}\int_{\Omega_j} c\,(S\phi)_x\,\mathrm{d}x\\
&\qquad\quad+\frac{1}{2}\sum_{j=1}^{N}\overline{c}_{j+1/2}S^-_{j+1/2}\phi^-_{j+1/2}-\frac{1}{2}\sum_{j=1}^{N}\overline{c}_{j-1/2}S^+_{j-1/2}\phi^+_{j-1/2}
\end{aligned} \tag{2.9}$$

for all $\phi\in X^p_{\Delta x}(\Omega)$,

$$\begin{aligned}
&\sum_{j=1}^{N}\int_{\Omega_j} S_t\eta\mathrm{d}x-\sum_{j=1}^{N}\int_{\Omega_j} cS\eta_x\mathrm{d}x+\sum_{j=1}^{N}\overline{c}_{j+1/2}\overline{S}_{j+1/2}\eta^-_{j+1/2}-\sum_{j=1}^{N}\overline{c}_{j-1/2}\overline{S}_{j-1/2}\eta^+_{j-1/2}\\
&\qquad=\frac{1}{2}\sum_{j=1}^{N}\int_{\Omega_j} c\,(R\eta)_x\,\mathrm{d}x-\frac{1}{2}\sum_{j=1}^{N}\overline{c}_{j+1/2}R^-_{j+1/2}\eta^-_{j+1/2}\\
&\qquad\quad+\frac{1}{2}\sum_{j=1}^{N}\overline{c}_{j-1/2}R^+_{j-1/2}\eta^+_{j-1/2}-\frac{1}{2}\sum_{j=1}^{N}\int_{\Omega_j} c\,(S\eta)_x\,\mathrm{d}x\\
&\qquad\quad+\frac{1}{2}\sum_{j=1}^{N}\overline{c}_{j+1/2}S^-_{j+1/2}\eta^-_{j+1/2}-\frac{1}{2}\sum_{j=1}^{N}\overline{c}_{j-1/2}S^+_{j-1/2}\eta^+_{j-1/2}
\end{aligned} \tag{2.10}$$

for all $\eta\in X^p_{\Delta x}(\Omega)$ and

$$\sum_{j=1}^{N}\int_{\Omega_j}\psi_t\,\zeta\mathrm{d}x=\sum_{j=1}^{N}\int_{\Omega_j}\frac{R+S}{2}\,\zeta\,\mathrm{d}x, \tag{2.11}$$

for all $\zeta\in X^p_{\Delta x}(\Omega)$.

The energy conservative property of this semi-discrete scheme is presented in the following theorem:

Proposition 2.1 (Energy conservation)**.** *Let $R, S \in X^p_{\Delta x}(\Omega)$ be a numerical solution of the semi-discrete scheme* (2.9)–(2.11) *with periodic boundary conditions. We then have*

$$\left(\sum_{j=1}^{N}\int_{\Omega_j}\frac{R^2+S^2}{2}\,\mathrm{d}x\right)_t = 0. \tag{2.12}$$

Proof. Since R and S are a numerical solution then (2.9) and (2.10) hold for any functions $\phi, \eta \in X^p_{\Delta x}(\Omega)$. In particular, they hold for the choice $\phi = R$ and $\eta = S$. We can then calculate

$$\begin{aligned}\sum_{j=1}^{N}\int_{\Omega_j} R_t R\mathrm{d}x = &-\frac{1}{2}\sum_{j=1}^{N}\int_{\Omega_j} c\,(SR)_x\,\mathrm{d}x + \frac{1}{2}\sum_{j=1}^{N}\overline{c}_{j+1/2}R^+_{j+1/2}R^-_{j+1/2}\\ &-\frac{1}{2}\sum_{j=1}^{N}\overline{c}_{j-1/2}R^-_{j-1/2}R^+_{j-1/2} + \frac{1}{2}\sum_{j=1}^{N}\overline{c}_{j+1/2}S^-_{j+1/2}R^-_{j+1/2}\\ &-\frac{1}{2}\sum_{j=1}^{N}\overline{c}_{j-1/2}S^+_{j-1/2}R^+_{j-1/2}\end{aligned} \tag{2.13}$$

and

$$\begin{aligned}\sum_{j=1}^{N}\int_{\Omega_j} S_t S\mathrm{d}x = &\frac{1}{2}\sum_{j=1}^{N}\int_{\Omega_j} c\,(SR)_x\,\mathrm{d}x - \frac{1}{2}\sum_{j=1}^{N}\overline{c}_{j+1/2}S^+_{j+1/2}S^-_{j+1/2}\\ &+\frac{1}{2}\sum_{j=1}^{N}\overline{c}_{j-1/2}S^-_{j-1/2}S^+_{j-1/2} - \frac{1}{2}\sum_{j=1}^{N}\overline{c}_{j+1/2}S^-_{j+1/2}R^-_{j+1/2}\\ &+\frac{1}{2}\sum_{j=1}^{N}\overline{c}_{j-1/2}S^+_{j-1/2}R^+_{j-1/2}.\end{aligned} \tag{2.14}$$

Putting these together we obtain

$$\begin{aligned}\left(\sum_{j=1}^{N}\int_{\Omega_j}\frac{R^2+S^2}{2}\,\mathrm{d}x\right)_t &= \sum_{j=1}^{N}\int_{\Omega_j}\left(RR_t + SS_t\right)\,\mathrm{d}x\\ &= \frac{1}{2}\sum_{j=1}^{N}\overline{c}_{j+1/2}\left(R^+_{j+1/2}R^-_{j+1/2} - S^+_{j+1/2}S^-_{j+1/2}\right)\\ &\quad -\frac{1}{2}\sum_{j=1}^{N}\overline{c}_{j-1/2}\left(R^-_{j-1/2}R^+_{j-1/2} - S^-_{j-1/2}S^+_{j-1/2}\right)\\ &= \frac{1}{2}\overline{c}_{N+1/2}\left(R^+_{N+1/2}R^-_{N+1/2} - S^+_{N+1/2}S^-_{N+1/2}\right)\\ &\quad -\frac{1}{2}\overline{c}_{1/2}\left(R^-_{1/2}R^+_{1/2} - S^-_{1/2}S^+_{1/2}\right) = 0,\end{aligned} \tag{2.15}$$

where we have used the periodic boundary conditions in the last equality. □

Remark 2.1. *Proposition* 2.1 *and similar results to follow are presented for periodic boundary conditions. Naturally, these results also hold when the numerical solution decays at the boundary.*

2.5. **Energy dissipating Scheme Based On System of Riemann Invariants.** We expect the above designed energy conservative scheme (2.9)–(2.11) to approximate a conservative solution of the underlying system (1.3). In order to be able to approximate a dissipative solution of (1.3), we add *numerical viscosity* (scaled by the maximum wave speed) as well as a *shock capturing operator* (similar to Barth [4]) to the energy conservative scheme (2.9)–(2.11). We propose the following modification of the energy conservative scheme (2.9)–(2.11):

Denoting

$$s_{j+1/2} = \max\{c^-_{j+1/2}, c^+_{j+1/2}\}$$

for the maximal local wave velocity, a dissipative version of the DG scheme is then given by the following: Find $R, S, \psi \in X^p_{\Delta x}(\Omega)$ such that

(2.16)

$$\begin{aligned}
\sum_{j=1}^{N}\int_{\Omega_j} R_t\phi \mathrm{d}x + \sum_{j=1}^{N}\int_{\Omega_j} cR\phi_x \mathrm{d}x - \sum_{j=1}^{N}\underbrace{\left(\left(\overline{c}_{j+1/2}\overline{R}_{j+1/2} + \frac{1}{2}s_{j+1/2}[\![R]\!]_{j+1/2}\right)\right.}_{\text{Diffusive flux}}\phi^-_{j+1/2} \\
+ \sum_{j=1}^{N}\underbrace{\left.\left(\overline{c}_{j-1/2}\overline{R}_{j-1/2} + \frac{1}{2}s_{j-1/2}[\![R]\!]_{j-1/2}\right)\right.}_{\text{Diffusive flux}}\phi^+_{j-1/2} \\
= \frac{1}{2}\sum_{j=1}^{N}\int_{\Omega_j} c\left(R\phi\right)_x \mathrm{d}x - \frac{1}{2}\sum_{j=1}^{N}\overline{c}_{j+1/2}R^-_{j+1/2}\phi^-_{j+1/2} \\
+ \frac{1}{2}\sum_{j=1}^{N}\overline{c}_{j-1/2}R^+_{j-1/2}\phi^+_{j-1/2} - \frac{1}{2}\sum_{j=1}^{N}\int_{\Omega_j} c\left(S\phi\right)_x \mathrm{d}x \\
+ \frac{1}{2}\sum_{j=1}^{N}\overline{c}_{j+1/2}S^-_{j+1/2}\phi^-_{j+1/2} - \frac{1}{2}\sum_{j=1}^{N}\overline{c}_{j-1/2}S^+_{j-1/2}\phi^+_{j-1/2} - \underbrace{\sum_{j=1}^{N}\varepsilon_j\int_{\Omega_j} R_x\phi_x \mathrm{d}x}_{\text{shock capturing operator}}
\end{aligned}$$

for all $\phi \in X^p_{\Delta x}(\Omega)$,

(2.17)

$$\begin{aligned}
\sum_{j=1}^{N}\int_{\Omega_j} S_t\eta \mathrm{d}x - \sum_{j=1}^{N}\int_{\Omega_j} cS\eta_x \mathrm{d}x + \sum_{j=1}^{N}\underbrace{\left(\overline{c}_{j+1/2}\overline{S}_{j+1/2} - \frac{1}{2}s_{j+1/2}[\![S]\!]_{j+1/2}\right)}_{\text{Diffusive flux}}\eta^-_{j+1/2} \\
- \sum_{j=1}^{N}\underbrace{\left(\overline{c}_{j-1/2}\overline{S}_{j-1/2} - \frac{1}{2}s_{j-1/2}[\![S]\!]_{j-1/2}\right)}_{\text{Diffusive flux}}\eta^+_{j-1/2} \\
= \frac{1}{2}\sum_{j=1}^{N}\int_{\Omega_j} c\left(R\eta\right)_x \mathrm{d}x - \frac{1}{2}\sum_{j=1}^{N}\overline{c}_{j+1/2}R^-_{j+1/2}\eta^-_{j+1/2} \\
+ \frac{1}{2}\sum_{j=1}^{N}\overline{c}_{j-1/2}R^+_{j-1/2}\eta^+_{j-1/2} - \frac{1}{2}\sum_{j=1}^{N}\int_{\Omega_j} c\left(S\eta\right)_x \mathrm{d}x \\
+ \frac{1}{2}\sum_{j=1}^{N}\overline{c}_{j+1/2}S^-_{j+1/2}\eta^-_{j+1/2} - \frac{1}{2}\sum_{j=1}^{N}\overline{c}_{j-1/2}S^+_{j-1/2}\eta^+_{j-1/2} - \underbrace{\sum_{j=1}^{N}\varepsilon_j\int_{\Omega_j} S_x\eta_x \mathrm{d}x}_{\text{shock capturing operator}}
\end{aligned}$$

for all $\eta \in X^p_{\Delta x}(\Omega)$ and

$$\sum_{j=1}^{N}\int_{\Omega_j} \psi_t\,\zeta \mathrm{d}x = \sum_{j=1}^{N}\int_{\Omega_j} \frac{R+S}{2}\,\zeta\,\mathrm{d}x, \tag{2.18}$$

for all $\zeta \in X^p_{\Delta x}(\Omega)$.

The scaling parameter ε_j in the *shock capturing operator* is given by

$$\varepsilon_j = \frac{\Delta x_j \, C \, \overline{\mathrm{Res}}}{\left(\int_{\Omega_j} (R_x^2 + S_x^2) \mathrm{d}x\right)^{1/2} + \Delta x_j^{\theta}} \tag{2.19}$$

where $C > 0$ is a constant, $\theta \geq 1/2$ and

$$\overline{\mathrm{Res}} = \left(\int_{\Omega_j} (\mathrm{Res})^2 \mathrm{d}x\right)^{1/2} \tag{2.20}$$

with

$$\mathrm{Res} = (R^2 + S^2)_t - \left(c(\psi)(R^2 - S^2)\right)_x . \tag{2.21}$$

Note that ε_j vanishes for smooth solutions.

We have the following theorem illustrating the energy dissipation associated with (2.16)–(2.18).

Proposition 2.2 (Energy stability)**.** *Let $R, S \in X^p_{\Delta x}(\Omega)$ be a numerical solution of the semi-discrete scheme* (2.16)–(2.18) *with periodic boundary conditions. We then have*

$$\left(\sum_{j=1}^{N} \int_{\Omega_j} \frac{R^2 + S^2}{2} \, \mathrm{d}x\right)_t \leq 0. \tag{2.22}$$

Proof. First, we calculate

$$\begin{aligned} \frac{1}{2}\sum_{j=1}^{N} s_{j+1/2} [\![R]\!]_{j+1/2} R^-_{j+1/2} - \frac{1}{2}\sum_{j=1}^{N} s_{j-1/2} [\![R]\!]_{j-1/2} R^+_{j-1/2} \\ + \frac{1}{2}\sum_{j=1}^{N} s_{j+1/2} [\![S]\!]_{j+1/2} S^-_{j+1/2} - \frac{1}{2}\sum_{j=1}^{N} s_{j-1/2} [\![S]\!]_{j-1/2} S^+_{j-1/2} \\ = -\frac{1}{2}\sum_{j=1}^{N} s_{j+1/2} \left([\![R]\!]^2_{j+1/2} + [\![S]\!]^2_{j+1/2} \right) \leq 0, \end{aligned} \tag{2.23}$$

since $s_{j+1/2} \geq 0$ for all j. Since R and S are a numerical solution, we can use (2.16)–(2.17) with $\phi = R$ and $\eta = S$, and proceed in a manner similar to the proof of Proposition 2.1 to estimate (2.24)

$$\begin{aligned}
\left(\sum_{j=1}^{N}\int_{\Omega_j}\frac{R^2+S^2}{2}\,\mathrm{d}x\right)_t &= \sum_{j=1}^{N}\int_{\Omega_j}(RR_t+SS_t)\,\mathrm{d}x \\
&= \frac{1}{2}\overline{c}_{N+1/2}\left(R^+_{N+1/2}R^-_{N+1/2}-S^+_{N+1/2}S^-_{N+1/2}\right) \\
&\quad -\frac{1}{2}\overline{c}_{1/2}\left(R^-_{1/2}R^+_{1/2}-S^-_{1/2}S^+_{1/2}\right)+\frac{1}{2}\sum_{j=1}^{N}s_{j+1/2}[\![R]\!]_{j+1/2}R^-_{j+1/2} \\
&\quad -\frac{1}{2}\sum_{j=1}^{N}s_{j-1/2}[\![R]\!]_{j-1/2}R^+_{j-1/2}+\frac{1}{2}\sum_{j=1}^{N}s_{j+1/2}[\![S]\!]_{j+1/2}S^-_{j+1/2} \\
&\quad -\frac{1}{2}\sum_{j=1}^{N}s_{j-1/2}[\![S]\!]_{j-1/2}S^+_{j-1/2}-\sum_{j=1}^{N}\varepsilon_j\int_{\Omega_j}(R_x^2+S_x^2)\,\mathrm{d}x \\
&= \frac{1}{2}\overline{c}_{N+1/2}\left(R^+_{N+1/2}R^-_{N+1/2}-S^+_{N+1/2}S^-_{N+1/2}\right) \\
&\quad -\frac{1}{2}\overline{c}_{1/2}\left(R^-_{1/2}R^+_{1/2}-S^-_{1/2}S^+_{1/2}\right)-\frac{1}{2}\sum_{j=1}^{N}s_{j+1/2}\left([\![R]\!]^2_{j+1/2}+[\![S]\!]^2_{j+1/2}\right) \\
&\quad -\sum_{j=1}^{N}\varepsilon_j\int_{\Omega_j}(R_x^2+S_x^2)\,\mathrm{d}x\leq 0,
\end{aligned}$$

where we have used the compact support in the last inequality. □

Hence, the scheme (2.16)–(2.18) is energy stable (dissipating) and we expect it to converge to a dissipative solution of (1.3) as the mesh is refined. We remark that energy dissipation results from adding *numerical viscosity* (scaled by the maximum wave speed) and a *shock capturing operator* to the energy conservative scheme (2.9)–(2.11).

2.6. **An alternative first-order system.** It is easy to check that the variational wave equation (1.3) can be rewritten as a first-order system by introducing the independent variables:

$$\begin{aligned} v &:= \psi_t \\ w &:= c(\psi)\psi_x \end{aligned}$$

Again, for smooth solutions, equation (1.3) is equivalent to the following system for (v, w, ψ):

$$\begin{cases} v_t-(c(\psi)w)_x=-c_x(\psi)w \\ w_t-(c(\psi)v)_x=0 \\ \psi_t=v \end{cases} \tag{2.25}$$

Furthermore, the energy associated with the above equation is

$$\mathcal{E}(t)=\int_{\mathbb{R}}\left(v^2+w^2\right)dx. \tag{2.26}$$

Again, we can check that smooth solutions of (2.25) preserve this energy. Weak solutions can be either energy conservative or energy dissipative.

2.7. **Variational formulation.** As before, we seek an approximation (v, w, ψ) of (2.25) such that for each $t \in [0, T]$, v, w, and ψ belong to finite dimensional space

$$X^p_{\Delta x}(\Omega)=\left\{u\in L^2(\Omega): u|_{\Omega_j}\text{ polynomial of degree}\leq p\right\}.$$

The variational form is derived by multiplying the strong form (2.25) with test functions $\phi, \eta, \zeta \in X^p_{\Delta x}(\Omega)$ and integrating over each element separately. After using integration-by-parts, we obtain

$$\begin{aligned}(2.27)\quad &\sum_{j=1}^{N}\int_{\Omega_j} v_t\,\phi \mathrm{d}x + \sum_{j=1}^{N}\int_{\Omega_j} c(\psi) w\phi_x\,\mathrm{d}x - \sum_{j=1}^{N}(cw)_{j+1/2}\phi^-_{j+1/2} + \sum_{j=1}^{N}(cw)_{j-1/2}\phi^+_{j-1/2} \\ &\qquad = \sum_{j=1}^{N}\int_{\Omega_j} c(\psi)\,(w\phi)_x\,\mathrm{d}x - \sum_{j=1}^{N}(c)_{j+1/2}w^-_{j+1/2}\phi^-_{j+1/2} + \sum_{j=1}^{N}(c)_{j-1/2}w^+_{j-1/2}\phi^+_{j-1/2}\end{aligned}$$

and

$$(2.28)\quad \sum_{j=1}^{N}\int_{\Omega_j} w_t\,\eta \mathrm{d}x + \sum_{j=1}^{N}\int_{\Omega_j} c(\psi) v\eta_x\,\mathrm{d}x - \sum_{j=1}^{N}(cv)_{j+1/2}\eta^-_{j+1/2} + \sum_{j=1}^{N}(cv)_{j-1/2}\eta^+_{j-1/2} \;=\; 0,$$

and

$$(2.29)\qquad \sum_{j=1}^{N}\int_{\Omega_j} \psi_t\,\zeta \mathrm{d}x = \sum_{j=1}^{N}\int_{\Omega_j} v\,\zeta\,\mathrm{d}x.$$

As before, the numerical fluxes $(cv)_{j+1/2}$, $(cw)_{j+1/2}$ and $(c)_{j+1/2}$ all need to be determined.

2.8. **Energy Preserving Scheme.** As before, for a conservative scheme, we use the numerical flux

$$(c)_{j\pm1/2} = \overline{c}_{j\pm1/2} \quad \text{and} \quad (cf)_{j\pm1/2} = \overline{c}_{j\pm1/2}\overline{f}_{j\pm1/2}.$$

Then, for the vw-formulation the DG scheme becomes: Find $v, w, \psi \in X^p_{\Delta x}(\Omega)$ such that

$$\begin{aligned}(2.30)\quad &\sum_{j=1}^{N}\int_{\Omega_j} v_t\,\phi \mathrm{d}x + \sum_{j=1}^{N}\int_{\Omega_j} c(\psi) w\phi_x\,\mathrm{d}x - \sum_{j=1}^{N}\overline{c}_{j+1/2}\overline{w}_{j+1/2}\phi^-_{j+1/2} + \sum_{j=1}^{N}\overline{c}_{j-1/2}\overline{w}_{j-1/2}\phi^+_{j-1/2} \\ &\qquad = \sum_{j=1}^{N}\int_{\Omega_j} c(\psi)\,(w\phi)_x\,\mathrm{d}x - \sum_{j=1}^{N}\overline{c}_{j+1/2}w^-_{j+1/2}\phi^-_{j+1/2} + \sum_{j=1}^{N}\overline{c}_{j-1/2}w^+_{j-1/2}\phi^+_{j-1/2}\end{aligned}$$

and

$$(2.31)\quad \sum_{j=1}^{N}\int_{\Omega_j} w_t\,\eta \mathrm{d}x + \sum_{j=1}^{N}\int_{\Omega_j} c(\psi) v\eta_x\,\mathrm{d}x - \sum_{j=1}^{N}\overline{c}_{j+1/2}\overline{v}_{j+1/2}\eta^-_{j+1/2} + \sum_{j=1}^{N}\overline{c}_{j-1/2}\overline{v}_{j-1/2}\eta^+_{j-1/2} \;=\; 0,$$

and

$$(2.32)\qquad \sum_{j=1}^{N}\int_{\Omega_j} \psi_t\,\zeta \mathrm{d}x = \sum_{j=1}^{N}\int_{\Omega_j} v\,\zeta\,\mathrm{d}x,$$

for all $\phi, \eta, \zeta \in X^p_{\Delta x}(\Omega)$.

We have the following theorem for the scheme:

Proposition 2.3 (Energy conservation)**.** *Let $v, w \in X^p_{\Delta x}(\Omega)$ be a numerical solution of the semi-discrete scheme* (2.30)–(2.32) *with periodic boundary conditions. We then have*

$$(2.33)\qquad \left(\sum_{j=1}^{N}\int_{\Omega_j}\left(v^2 + w^2\right)\mathrm{d}x\right)_t = 0.$$

Proof. Since v and w are a numerical solution then (2.30) and (2.31) hold for any functions $\phi, \eta \in X^p_{\Delta x}(\Omega)$. In particular, they hold for the choice $\phi = v$ and $\eta = w$. We can then calculate

(2.34)
$$\begin{aligned}\left(\sum_{j=1}^{N}\int_{\Omega_j}\left(v^2+w^2\right)\mathrm{d}x\right)_t &= 2\sum_{j=1}^{N}\int_{\Omega_j}\left(v_t v + w_t w\right)\mathrm{d}t \\ &= 2\sum_{j=1}^{N}\Big(\overline{c}_{j+1/2}\left(\overline{w}_{j+1/2}v^-_{j+1/2} - w^-_{j+1/2}v^-_{j+1/2} + \overline{v}_{j+1/2}w^-_{j+1/2}\right) \\ &\quad + \overline{c}_{j-1/2}\left(-\overline{w}_{j-1/2}v^+_{j-1/2} + w^+_{j-1/2}v^+_{j-1/2} - \overline{v}_{j-1/2}w^+_{j-1/2}\right)\Big) \\ &= 2\sum_{j=1}^{N}\overline{c}_{j+1/2}\left(-\overline{w}_{j+1/2}[\![v]\!]_{j+1/2} + [\![wv]\!]_{j+1/2} - \overline{v}_{j+1/2}[\![w]\!]_{j+1/2}\right) = 0,\end{aligned}$$

where we have used the periodic boundary conditions and the identity (2.1). □

2.9. **Energy Dissipating Scheme.** In-order to approximate dissipative solutions, we again add some numerical viscosity and a shock capturing operator to the energy conservative scheme (2.30)–(2.32) to obtain the following dissipative scheme: Find $v, w, \psi \in X^p_{\Delta x}(\Omega)$ such that

(2.35)
$$\begin{aligned}&\sum_{j=1}^{N}\int_{\Omega_j} v_t\,\phi\mathrm{d}x + \sum_{j=1}^{N}\int_{\Omega_j} c(\psi)w\phi_x\,\mathrm{d}x - \sum_{j=1}^{N}\left(\overline{c}_{j+1/2}\overline{w}_{j+1/2} + \frac{1}{2}s_{j+1/2}[\![v]\!]_{j+1/2}\right)\phi^-_{j+1/2} \\ &\qquad + \sum_{j=1}^{N}\left(\overline{c}_{j-1/2}\overline{w}_{j-1/2} + \frac{1}{2}s_{j-1/2}[\![v]\!]_{j-1/2}\right)\phi^+_{j-1/2} \\ &= \sum_{j=1}^{N}\int_{\Omega_j} c(\psi)\left(w\phi\right)_x\mathrm{d}x - \sum_{j=1}^{N}\overline{c}_{j+1/2}w^-_{j+1/2}\phi^-_{j+1/2} + \sum_{j=1}^{N}\overline{c}_{j-1/2}w^+_{j-1/2}\phi^+_{j-1/2} - \sum_{j=1}^{N}\varepsilon_j\int_{\Omega_j} v_x\phi_x\mathrm{d}x.\end{aligned}$$

for all $\phi \in X^p_{\Delta x}(\Omega)$,

$$\begin{aligned}&\sum_{j=1}^{N}\int_{\Omega_j} w_t\,\eta\mathrm{d}x + \sum_{j=1}^{N}\int_{\Omega_j} c(\psi)v\eta_x\,\mathrm{d}x - \sum_{j=1}^{N}\left(\overline{c}_{j+1/2}\overline{v}_{j+1/2} + \frac{1}{2}s_{j+1/2}[\![w]\!]_{j+1/2}\right)\eta^-_{j+1/2} \\ &\qquad + \sum_{j=1}^{N}\left(\overline{c}_{j-1/2}\overline{v}_{j-1/2} + \frac{1}{2}s_{j-1/2}[\![w]\!]_{j-1/2}\right)\eta^+_{j-1/2} = -\sum_{j=1}^{N}\varepsilon_j\int_{\Omega_j} w_x\eta_x\mathrm{d}x,\end{aligned} \tag{2.36}$$

for all $\eta \in X^p_{\Delta x}(\Omega)$ and

$$\sum_{j=1}^{N}\int_{\Omega_j}\psi_t\,\zeta\mathrm{d}x = \sum_{j=1}^{N}\int_{\Omega_j} v\,\zeta\,\mathrm{d}x, \tag{2.37}$$

for all $\zeta \in X^p_{\Delta x}(\Omega)$.

Expressed in v and w, the parameter ε_j is given by

$$\varepsilon_j = \frac{\Delta x_j\, C\,\overline{\mathrm{Res}}}{\left(\int_{\Omega_j}(v_x^2 + w_x^2)\mathrm{d}x\right)^{1/2} + \Delta x_j^{\theta}} \tag{2.38}$$

where $C > 0$ is a constant, $\theta \geq 1/2$ and

$$\overline{\mathrm{Res}} = \left(\int_{\Omega_j}(\mathrm{Res})^2\mathrm{d}x\right)^{1/2}, \quad \mathrm{Res} = \left(v^2+w^2\right)_t - \left(2c(\psi)vw\right)_x. \tag{2.39}$$

We show that the above scheme dissipates energy in the following theorem:

Proposition 2.4 (Energy stability)**.** *Let $v, w \in X^p_{\Delta x}(\Omega)$ be a numerical solution of the semi-discrete scheme* (2.35)–(2.37) *with periodic boundary conditions. We then have*

$$\left(\sum_{j=1}^{N}\int_{\Omega_j}\frac{v^2+w^2}{2}\,\mathrm{d}x\right)_t \le 0. \tag{2.40}$$

Proof. Since v and w are a numerical solution, we can use (2.35)–(2.36) with $\phi = v$ and $\eta = w$ and estimate

(2.41)

$$\begin{aligned}
\left(\sum_{j=1}^{N}\int_{\Omega_j}\frac{v^2+w^2}{2}\,\mathrm{d}x\right)_t &= \sum_{j=1}^{N}\int_{\Omega_j}(v_t v + w_t w)\,\mathrm{d}x \\
&= \sum_{j=1}^{N}\Big(\overline{c}_{j+1/2}\left(\overline{w}_{j+1/2}v^-_{j+1/2} - w^-_{j+1/2}v^-_{j+1/2} + \overline{v}_{j+1/2}w^-_{j+1/2}\right) \\
&\quad + \overline{c}_{j-1/2}\left(-\overline{w}_{j-1/2}v^+_{j-1/2} + w^+_{j-1/2}v^+_{j-1/2} - \overline{v}_{j-1/2}w^+_{j-1/2}\right)\Big) \\
&\quad + \frac{1}{2}\sum_{j=1}^{N}\Big(s_{j+1/2}\left(\llbracket v\rrbracket_{j+1/2}v^-_{j+1/2} + \llbracket w\rrbracket_{j+1/2}w^-_{j+1/2}\right) \\
&\quad - s_{j-1/2}\left(\llbracket v\rrbracket_{j-1/2}v^+_{j-1/2} + \llbracket w\rrbracket_{j-1/2}w^+_{j-1/2}\right)\Big) - \sum_{j=1}^{N}\varepsilon_j\int_{\Omega_j}\left(v_x^2+w_x^2\right)\mathrm{d}x \\
&= \sum_{j=1}^{N}\overline{c}_{j+1/2}\left(-\overline{w}_{j+1/2}\llbracket v\rrbracket_{j+1/2} + \llbracket wv\rrbracket_{j+1/2} - \overline{v}_{j+1/2}\llbracket w\rrbracket_{j+1/2}\right) \\
&\quad + \frac{1}{2}\sum_{j=1}^{N}\Big(s_{j+1/2}\left(\llbracket v\rrbracket_{j+1/2}v^-_{j+1/2} + \llbracket w\rrbracket_{j+1/2}w^-_{j+1/2}\right) \\
&\quad - s_{j-1/2}\left(\llbracket v\rrbracket_{j-1/2}v^+_{j-1/2} + \llbracket w\rrbracket_{j-1/2}w^+_{j-1/2}\right)\Big) - \sum_{j=1}^{N}\varepsilon_j\int_{\Omega_j}\left(v_x^2+w_x^2\right)\mathrm{d}x \\
&= -\frac{1}{2}\sum_{j=1}^{N}s_{j+1/2}\left(\llbracket v\rrbracket^2_{j+1/2} + \llbracket w\rrbracket^2_{j+1/2}\right) - \sum_{j=1}^{N}\varepsilon_j\int_{\Omega_j}\left(v_x^2+w_x^2\right)\mathrm{d}x \le 0,
\end{aligned}$$

where we have used the identities (2.1) as well as the periodic boundary conditions. □

3. Details on the Implementation

All numerical experiments in this article are performed with an uniform grid spacing $\Delta x_j = \Delta x$. The time step is determined according to

$$\Delta t = 0.1\frac{\Delta x}{\sup\limits_{\psi\in[0,\pi)} c(\psi)}.$$

Furthermore, for the shock capturing operator, we use $C = 0.1$ and $\theta = 1$.

3.1. Choice of basis.

Let $\tilde{\Omega} = [-1, 1]$ be the usual reference domain. As a basis for $\mathbb{P}^p(\tilde{\Omega})$, the space of polynomials on $\tilde{\Omega}$ of degree at most p, we use the Lagrangian interpolants

$$\ell_k(\xi) = \prod_{\substack{0\le j\le p\\ j\neq k}}\frac{\xi-\xi_j}{\xi_k-\xi_j}, \tag{3.1}$$

where ξ_j, $j = 1, \dots, p$, are the interpolation points. Note that the Lagrangian interpolants satisfy $\ell_i(\xi_\alpha) = \delta_{i\alpha}$ and thus the discrete orthogonality property

$$\int_{\Omega_j} \ell_j(\xi)\ell_k(\xi)\mathrm{d}\xi = \sum_{\alpha=0}^{p} \rho_\alpha \ell_j(\xi_\alpha)\ell_k(\xi_\alpha) = \rho_j \delta_{jk}, \tag{3.2}$$

where ρ_α, $\alpha = 0, \dots, p$, are quadrature weights.

We introduce the necessary notation required for representing grid functions and quadrature formulas in terms of the basis (3.1). Defining the mapping $\eta_j : \Omega_j \to \tilde{\Omega}$ by

$$\eta_j(x) = 2\frac{x - x_j}{\Delta x}, \tag{3.3}$$

a function $f : \Omega \times [0, T] \to \mathbb{R}$ with $f(\cdot, t) \in X^p_{\Delta x}(\Omega)$ can be written as

$$f(x, t) = \sum_{j=1}^{N} \chi_{\Omega_j}(x) \sum_{k=0}^{p} f_j^{(k)}(t)\ell_k(\eta_j(x)), \tag{3.4}$$

in terms of time dependent coefficients $f_j^{(k)}(t)$. Moreover, we can use the shorthand notation

$$\tilde{f}_j(\xi, t) = f(\eta_j^{-1}(\xi), t) \tag{3.5}$$

for evaluating f on the reference domain. In addition, it is convenient to denote $c_j(\xi) = c\left(\tilde{\psi}_j(\xi)\right)$.

The integrals appearing in the DG formulation must be approximated using quadrature. Let $f \in X^p_{\Delta x}(\Omega)$ and represented by (3.4). We can then readily calculate the approximations

$$\begin{aligned}\int_{\Omega_j} f(x,t)_t \ell_i(\eta_j(x))\,\mathrm{d}x &= \frac{\Delta x}{2}\int_{\tilde{\Omega}} \left(\tilde{f}_j\right)_t \ell_i(\xi)\,\mathrm{d}\xi = \frac{\Delta x}{2}\sum_{\alpha=0}^{p}\rho_\alpha\left(\sum_{k=0}^{p}\left(f_j^{(k)}\right)_t \ell_k(\xi_\alpha)\right)\ell_i(\xi_\alpha)\\ &= \frac{\Delta x}{2}\sum_{\alpha=0}^{p}\rho_\alpha\left(\sum_{k=0}^{p}\left(f_j^{(k)}\right)_t \delta_{k\alpha}\right)\delta_{i\alpha} = \frac{\Delta x}{2}\rho_i\left(f_j^{(i)}\right)_t,\end{aligned} \tag{3.6}$$

$$\begin{aligned}\int_{\Omega_j} c(\psi)f(x,t)\ell_i(\eta_j(x))_x\,\mathrm{d}x &= \int_{\tilde{\Omega}} c_j(\xi)\tilde{f}_j(\xi,t)\ell_i'(\xi)\,\mathrm{d}\xi = \sum_{\alpha=0}^{p}\rho_\alpha c_j(\xi_\alpha)\left(\sum_{k=0}^{p} f_j^{(k)}\ell_k(\xi_\alpha)\right)\ell_i'(\xi_\alpha)\\ &= \sum_{\alpha=0}^{p}\rho_\alpha c_j(\xi_\alpha)\left(\sum_{k=0}^{p} f_j^{(k)}\delta_{k\alpha}\right)\ell_i'(\xi_\alpha) = \sum_{\alpha=0}^{p}\rho_\alpha c_j(\xi_\alpha) f_j^{(\alpha)} D_{\alpha i},\end{aligned} \tag{3.7}$$

$$\begin{aligned}\int_{\Omega_j} c(\psi)f(x,t)_x\ell_i(\eta_j(x))\,\mathrm{d}x &= \int_{\tilde{\Omega}} c_j(\xi)\tilde{f}_j(\xi,t)_\xi\ell_i(\xi)\,\mathrm{d}\xi = \sum_{\alpha=0}^{p}\rho_\alpha c_j(\xi_\alpha)\left(\sum_{k=0}^{p} f_j^{(k)}\ell_k'(\xi_\alpha)\right)\ell_i(\xi_\alpha)\\ &= \sum_{\alpha=0}^{p}\rho_\alpha c_j(\xi_\alpha)\left(\sum_{k=0}^{p} f_j^{(k)}\ell_k'(\xi_\alpha)\right)\delta_{i\alpha} = \rho_i c_j(\xi_i)\sum_{k=0}^{p} f_j^{(k)} D_{ik},\end{aligned} \tag{3.8}$$

$$\int_{\Omega_j} f(x,t)_x\ell_i(\eta_j(x))_x\mathrm{d}x = \frac{2}{\Delta x}\int_{\tilde{\Omega}} \tilde{f}(\xi,t)_\xi\ell_i(\xi)_\xi\mathrm{d}\xi = \frac{2}{\Delta x_j}\sum_{\alpha=0}^{p}\sum_{k=0}^{p}\rho_\alpha f_j^{(k)} D_{\alpha k}D_{\alpha i}, \tag{3.9}$$

and

$$\int_{\Omega_j} (f(x,t)_x)^2\,\mathrm{d}x = \frac{2}{\Delta x}\sum_{\alpha=0}^{p}\rho_\alpha\left(\sum_{k=1}^{p} f_j^{(k)} D_{\alpha k}\right)^2, \tag{3.10}$$

where we have introduced the derivative matrix $D_{ij} = \ell_j'(\xi_i)$.

For the interpolation points ξ_α on the reference domain we use the Gauss–Lobatto–Legendre (GLL) points. This is a set of points particularly convenient for the implementation since they contain the end points. In this paper we will present numerical experiments for $p = 0, 1, 2, 3$.

The GLL points, weights, Lagrangian interpolants and their corresponding derivative matrices are omitted here, but can be found in Appendix A.

3.2. **Runge–Kutta time discretization.** The schemes derived in this paper are all in a semi-discrete form

$$u_t = f(t, u_{\Delta x}),$$

where $u_{\Delta x}$ is the discrete solution. The RKDG method utilizes the Runge–Kutta (RK) time marching scheme to advance the solution. Herein, the spatial accuracy in the semi-discrete scheme should be matched with an equally accurate RK scheme to obtain the desired order of accuracy for smooth solutions. Therefore, the following fifth-order RK algorithm was used in this work [25]: Let $u^n_{\Delta x}$ be the discrete solution at time t^n and let $\Delta t^n = t^{n+1} - t^n$. The solutions is then advanced according to

$$\begin{aligned}
k_1 &= f(t^n, u^n_{\Delta x}) \\
k_2 &= f\left(t^n + \frac{4\Delta t^n}{11}, u^n_{\Delta x} + \frac{4\Delta t^n}{11} k_1\right) \\
k_3 &= f\left(t^n + \frac{2\Delta t^n}{5}, u^n_{\Delta x} + \frac{\Delta t^n}{50}(9k_1 + 11k_2)\right) \\
k_4 &= f\left(t^n + \Delta t^n, u^n_{\Delta x} + \frac{\Delta t^n}{4}(-11k_2 + 15k_3)\right) \\
k_5 &= f\left(t^n + (6-\sqrt{6})\frac{\Delta t^n}{10}, u^n_{\Delta x} + \frac{\Delta t^n}{600}\left((81+9\sqrt{6})k_1 + (255-55\sqrt{6})k_3 + (24-14\sqrt{6})k_4\right)\right) \\
k_6 &= f\left(t^n + (6+\sqrt{6})\frac{\Delta t^n}{10}, u^n_{\Delta x} + \frac{\Delta t^n}{600}\left((81-9\sqrt{6})k_1 + (255+55\sqrt{6})k_3 + (24+14\sqrt{6})k_4\right)\right) \\
u^{n+1} &= u^n_{\Delta x} + \frac{1}{36}\Delta t^n\left(4k_1 + (16+\sqrt{6})k_5 + (16-\sqrt{6})k_6\right).
\end{aligned}$$

4. Numerical experiments

In the following, we perform numerical experiments to demonstrate the properties of the present DG schemes for $p = 0, 1, 2, 3$. Henceforth, the schemes (16 in total) will be named according to ⟨formulation⟩⟨p⟩⟨c/d⟩. For example, the piecewise linear conservative scheme using the RS formulation will be referred to as RS1c and the piecewise cubic dissipative scheme using the vw formulation will be referred to as vw3d.

4.1. **Order of convergence to manufactured solution.** One of the main attractions of the discontinuous Galerkin scheme is the easy construction of high-order methods. In the following, we numerically demonstrate the order of convergence for smooth solutions. As previously discussed, the non-linear variational wave equation exhibits blow up in finite time and thus no global smooth solutions are known. However, the order of accuracy can be obtained by using the method of manufactured solutions. If we assert that

$$\psi(x,t) = \sin(x-t) \tag{4.1}$$

then we can for the formulation (2.3) calculate the residual

$$\begin{aligned}
Q(x,t) &:= R_t - (c(\psi)R)_x + \frac{c_x(\psi)}{2}(R-S) \\
&= S_t + (c(\psi)S)_x + \frac{c_x(\psi)}{2}(R-S) = \sin(x-t)\left(c^2(\psi)-1\right) - c(\psi)c'(\psi)\cos^2(x-t).
\end{aligned} \tag{4.2}$$

Also, for the formulation (2.25) we have

$$v_t - c(\psi)w_x = Q(x,t) \tag{4.3}$$

TABLE 4.1. The order of convergence at $t = 1.0$ for the manufactured sine solution (4.1) for the RS formulation using $N = 20 \times 2^i$.

	i	4	5	6	7	8
RS0c	$e_{L^2}^{\Delta x}$	$2.279 \cdot 10^{-3}$	$5.698 \cdot 10^{-4}$	$1.424 \cdot 10^{-4}$	$3.561 \cdot 10^{-5}$	$8.901 \cdot 10^{-6}$
	rate	-	2.000	2.000	2.000	2.000
RS0d	$e_{L^2}^{\Delta x}$	$4.053 \cdot 10^{-2}$	$2.063 \cdot 10^{-2}$	$1.041 \cdot 10^{-2}$	$5.231 \cdot 10^{-3}$	$2.622 \cdot 10^{-3}$
	rate	-	0.974	0.986	0.993	0.996
RS1c	$e_{L^2}^{\Delta x}$	$3.925 \cdot 10^{-2}$	$1.962 \cdot 10^{-2}$	$9.811 \cdot 10^{-3}$	$4.906 \cdot 10^{-3}$	$2.453 \cdot 10^{-3}$
	rate	-	1.000	1.000	1.000	1.000
RS1d	$e_{L^2}^{\Delta x}$	$3.590 \cdot 10^{-3}$	$9.068 \cdot 10^{-4}$	$2.275 \cdot 10^{-4}$	$5.695 \cdot 10^{-5}$	$1.425 \cdot 10^{-5}$
	rate	-	1.985	1.995	1.998	1.999
RS2c	$e_{L^2}^{\Delta x}$	$1.820 \cdot 10^{-5}$	$2.255 \cdot 10^{-6}$	$2.812 \cdot 10^{-7}$	$3.513 \cdot 10^{-8}$	$4.390 \cdot 10^{-9}$
	rate	-	3.013	3.003	3.001	3.000
RS2d	$e_{L^2}^{\Delta x}$	$2.090 \cdot 10^{-5}$	$2.594 \cdot 10^{-6}$	$3.235 \cdot 10^{-7}$	$4.040 \cdot 10^{-8}$	$5.049 \cdot 10^{-9}$
	rate	-	3.010	3.003	3.001	3.001
RS3c	$e_{L^2}^{\Delta x}$	$2.445 \cdot 10^{-6}$	$3.058 \cdot 10^{-7}$	$3.822 \cdot 10^{-8}$	$4.777 \cdot 10^{-9}$	$5.971 \cdot 10^{-10}$
	rate	-	2.999	3.000	3.000	3.000
RS3d	$e_{L^2}^{\Delta x}$	$2.577 \cdot 10^{-7}$	$1.609 \cdot 10^{-8}$	$1.005 \cdot 10^{-9}$	$6.282 \cdot 10^{-11}$	$3.926 \cdot 10^{-12}$
	rate	-	4.001	4.001	4.000	4.000

and

$$w_t - (c(\psi)v)_x = 0. \tag{4.4}$$

Thus, (4.1) will be a smooth solution to the problems

$$R_t - (c(\psi)R)_x = -\frac{c_x(\psi)}{2}(R - S) + Q(x,t)$$
$$S_t + (c(\psi)S)_x = -\frac{c_x(\psi)}{2}(R - S) + Q(x,t)$$

and

$$v_t - (c(\psi)w)_x = -c_x(\psi)w + Q(x,t)$$
$$w_t - (c(\psi)v)_x = 0,$$

which differ from the original problems only through the local source terms $Q(x,t)$. The spatial and temporal accuracy of the schemes can then be calculated by solving with the extra source terms, using periodic boundary conditions and approximating the error as

$$e_{L^2}^{\Delta x} = \left(\frac{\Delta x}{2} \sum_{j=1}^{N} \sum_{\alpha=0}^{p} \rho_\alpha \left| \sin(x_j^\alpha, t) - \psi_j^{\Delta x}(x_j^\alpha, t) \right|^2 \right)^{1/2}, \tag{4.5}$$

where $x_j^\alpha = x_0 + \Delta x \left(j + \frac{1}{2}\xi_\alpha \right)$.

Table 4.1 shows the error and the rate of convergence for the RS schemes and Table 4.2 for the vw schemes. The piecewise constant ($p = 0$) schemes demonstrate second order convergence. For odd polynomial orders p the conservative schemes exhibit sub-optimal convergence rates, a type of behavior that has been observed for the discontinuous Galerkin method when using central fluxes [29]. For the other schemes the order of convergence is optimal ($p + 1$).

4.2. **Gaussian initial data.** A basic test problem for the nonlinear variational wave equation is obtained by considering the smooth initial data

$$\psi(x,0) = \frac{\pi}{4} + \exp\left(-x^2\right), \tag{4.6}$$

$$\psi_t(x,0) = -c(\psi(x,0))\psi_x(x,0), \tag{4.7}$$

TABLE 4.2. The order of convergence at $t = 1.0$ for the manufactured sine solution (4.1) for the vw formulation using $N = 20 \times 2^i$.

	i	4	5	6	7	8
vw0c	$e_{L^2}^{\Delta x}$	$2.279 \cdot 10^{-3}$	$5.698 \cdot 10^{-4}$	$1.424 \cdot 10^{-4}$	$3.561 \cdot 10^{-5}$	$8.901 \cdot 10^{-6}$
	rate	-	2.000	2.000	2.000	2.000
vw0d	$e_{L^2}^{\Delta x}$	$5.294 \cdot 10^{-2}$	$2.676 \cdot 10^{-2}$	$1.345 \cdot 10^{-2}$	$6.746 \cdot 10^{-3}$	$3.380 \cdot 10^{-3}$
	rate	-	0.985	0.992	0.996	0.998
vw1c	$e_{L^2}^{\Delta x}$	$4.096 \cdot 10^{-2}$	$2.046 \cdot 10^{-2}$	$1.022 \cdot 10^{-2}$	$5.109 \cdot 10^{-3}$	$2.554 \cdot 10^{-3}$
	rate	-	1.002	1.001	1.000	1.000
vw1d	$e_{L^2}^{\Delta x}$	$3.590 \cdot 10^{-3}$	$9.068 \cdot 10^{-4}$	$2.275 \cdot 10^{-4}$	$5.695 \cdot 10^{-5}$	$1.425 \cdot 10^{-5}$
	rate	-	1.985	1.995	1.998	1.999
vw2c	$e_{L^2}^{\Delta x}$	$1.820 \cdot 10^{-5}$	$2.255 \cdot 10^{-6}$	$2.812 \cdot 10^{-7}$	$3.513 \cdot 10^{-8}$	$4.390 \cdot 10^{-9}$
	rate	-	3.013	3.003	3.001	3.000
vw2d	$e_{L^2}^{\Delta x}$	$1.852 \cdot 10^{-5}$	$2.296 \cdot 10^{-6}$	$2.863 \cdot 10^{-7}$	$3.575 \cdot 10^{-8}$	$4.468 \cdot 10^{-9}$
	rate	-	3.013	3.003	3.001	3.000
vw3c	$e_{L^2}^{\Delta x}$	$2.445 \cdot 10^{-6}$	$3.058 \cdot 10^{-7}$	$3.822 \cdot 10^{-8}$	$4.778 \cdot 10^{-9}$	$5.971 \cdot 10^{-10}$
	rate	-	2.999	3.000	3.000	3.000
vw3d	$e_{L^2}^{\Delta x}$	$2.577 \cdot 10^{-7}$	$1.609 \cdot 10^{-8}$	$1.005 \cdot 10^{-9}$	$6.282 \cdot 10^{-11}$	$3.926 \cdot 10^{-12}$
	rate	-	4.001	4.001	4.000	4.000

for $x \in \mathbb{R}$. This problem has been tested numerically in the literature [16, 20]. It is an example of an initial-value problem with smooth initial data that exhibits blow-up in finite time.

The initial data (4.6)–(4.7) was solved numerically using the vw schemes with $\alpha = 0.5$ and $\beta = 1.5$ for $t \in [0, 10]$ using $N = 1000$. Results for the RS schemes are similar, and are omitted here to avoid unnecessary redundancy. Figure 4.1 shows the results when using the conservative schemes and Figure 4.2 using the dissipative schemes. Also, Figures 4.3 and 4.4 show the evolutions of the auxiliary variables $v = \psi_t$ and $w = c(\psi)\psi_x$ for the conservative and dissipative piecewise cubic schemes, respectively. The results are consistent with those reported by Holden et al. [20]. Despite the initial data being smooth, the solution develops a singularity in ψ_x at around $t = 6$. After this time, spurious oscillations can be observed in the numerical solutions when using the conservative schemes. This effect is not present when using the dissipative schemes.

The schemes derived in this paper have been categorised into conservative and dissipative schemes. Figure 4.5 shows the evolution of the discrete energy

$$E = \sum_{j=1}^{N} \int_{\Omega_j} \frac{R^2 + S^2}{4} \mathrm{d}x = \frac{\Delta x}{8} \sum_{j=1}^{N} \sum_{k=0}^{p} \rho_k \left(\left(R_j^{(k)} \right)^2 + \left(S_j^{(k)} \right)^2 \right), \tag{4.8}$$

or alternatively for the vw formulation

$$E = \sum_{j=1}^{N} \int_{\Omega_j} \frac{v^2 + w^2}{2} \mathrm{d}x = \frac{\Delta x}{4} \sum_{j=1}^{N} \sum_{k=0}^{p} \rho_k \left(\left(v_j^{(k)} \right)^2 + \left(w_j^{(k)} \right)^2 \right), \tag{4.9}$$

for the Gaussian test problem. The results demonstrate clearly the difference between the dissipative and conservative schemes. Indeed, no significant change in the discrete energy can be observed for any of the conservative schemes. Conversely, the dissipative schemes all cause a reduction in the energy.

A key aspect of the nonlinear variational wave equation is the existence of both conservative and dissipative weak solutions. The schemes derived in this paper enables us to investigate this numerically. Figure 4.6 show the numerical solution to the Gaussian test problem with $\alpha = 0.5$ and $\beta = 4.5$ using the conservative (vw3c) and dissipative (vw3d) piecewise cubic schemes. The results clearly indicate that the solution, while initially smooth, develops a singularity at about $t = 5$ (see Fig. 4.6a). After the formation of the singularity we observe that the conservative and dissipative schemes give two distinct solutions, as shown in Figure 4.6b. Table 4.4 shows that the

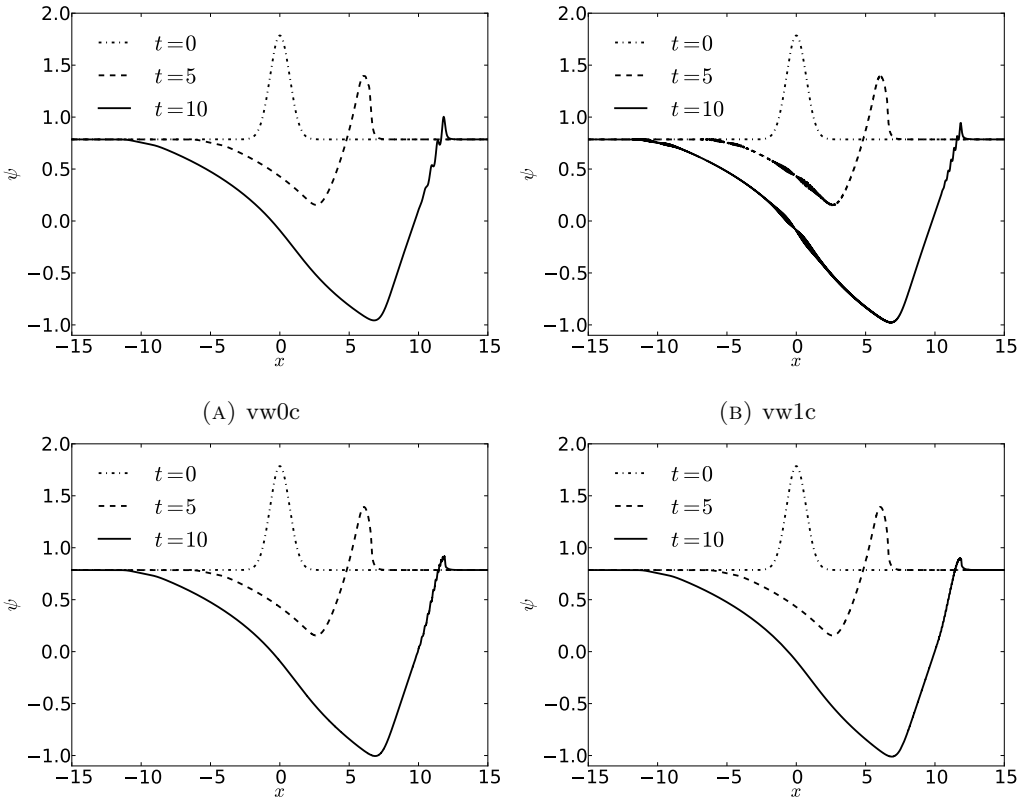

(A) vw0c (B) vw1c

(C) vw2c (D) vw3c

FIGURE 4.1. The numerical solution of the Gaussian test problem with $\alpha = 0.5$ and $\beta = 1.5$ using the conservative schemes based on the vw formulation with $N = 1000$.

TABLE 4.3. The error $\|\psi - \psi_{\text{ref}}\|_2$ for the vw schemes at $t = 1$ for the Gaussian test problem with $\alpha = 0.5$ and $\beta = 1.5$ using $N = 20 \times 2^i$. The reference solution was computed using the vw3c scheme with $N = 25000$.

i	3	4	5	6
vw0c	$7.221 \cdot 10^{-2}$	$3.176 \cdot 10^{-2}$	$1.528 \cdot 10^{-2}$	$7.561 \cdot 10^{-3}$
vw0d	$1.902 \cdot 10^{-1}$	$1.047 \cdot 10^{-1}$	$5.533 \cdot 10^{-2}$	$2.851 \cdot 10^{-2}$
vw1c	$8.465 \cdot 10^{-2}$	$4.180 \cdot 10^{-2}$	$2.083 \cdot 10^{-2}$	$1.041 \cdot 10^{-2}$
vw1d	$3.490 \cdot 10^{-2}$	$9.704 \cdot 10^{-3}$	$2.523 \cdot 10^{-3}$	$6.396 \cdot 10^{-4}$
vw2c	$7.566 \cdot 10^{-4}$	$7.650 \cdot 10^{-5}$	$9.288 \cdot 10^{-6}$	$1.151 \cdot 10^{-6}$
vw2d	$7.373 \cdot 10^{-4}$	$7.770 \cdot 10^{-5}$	$9.384 \cdot 10^{-6}$	$1.164 \cdot 10^{-6}$
vw3c	$5.547 \cdot 10^{-5}$	$6.870 \cdot 10^{-6}$	$8.568 \cdot 10^{-7}$	$1.070 \cdot 10^{-7}$
vw3d	$2.612 \cdot 10^{-5}$	$1.634 \cdot 10^{-6}$	$1.023 \cdot 10^{-7}$	$6.397 \cdot 10^{-9}$

rest of the conservative schemes indeed converge to the conservative reference solution shown in Figure 4.6b. Conversely, the dissipative schemes converge to the dissipative (dashed) solution in Figure 4.6b, as shown in Table 4.5. We note that in both cases the convergence is in N as well as in p. Also, as can be expected, after the blow up of ψ_x the rate of convergence is slower than for the smooth manufactured solution.

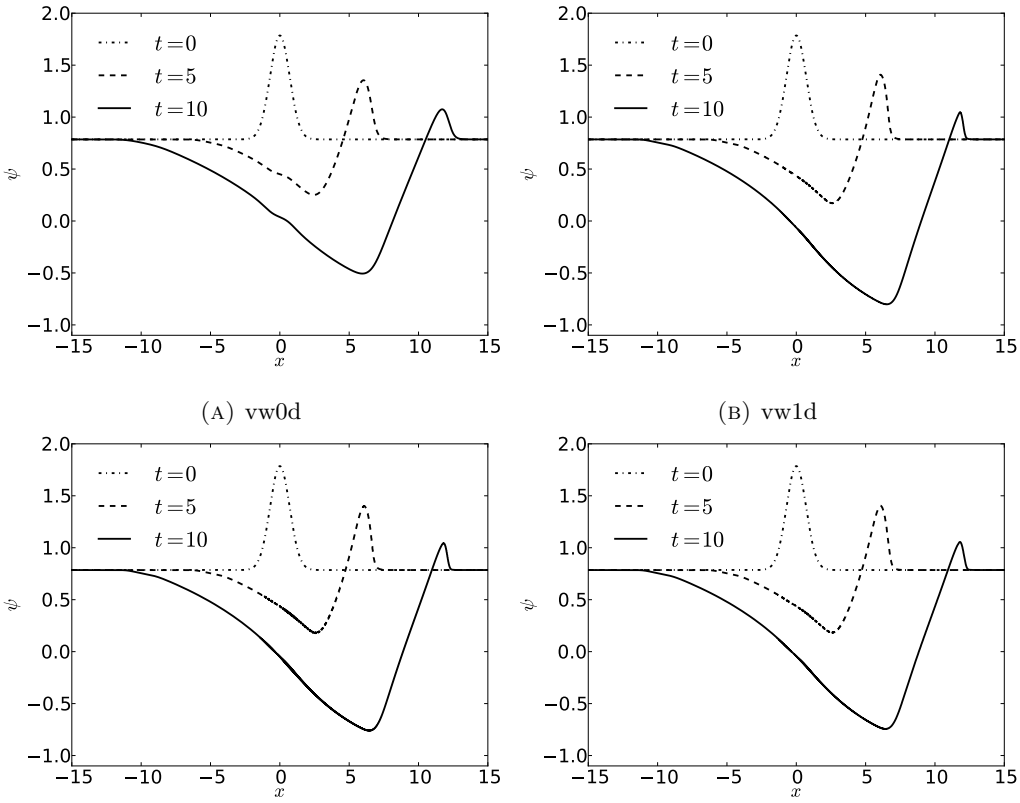

(A) vw0d (B) vw1d

(C) vw2d (D) vw3d

FIGURE 4.2. The numerical solution of the Gaussian test problem with $\alpha = 0.5$ and $\beta = 1.5$ using the dissipative schemes based on the vw formulation with $N = 1000$.

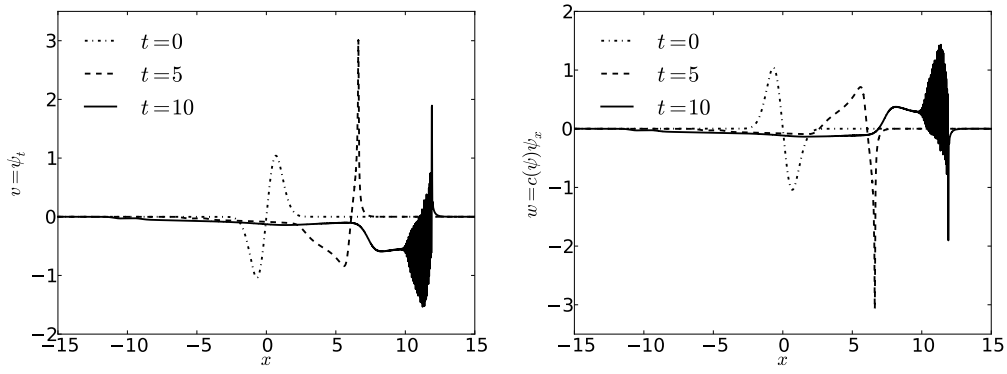

(A) v (B) w

FIGURE 4.3. The numerical solution of the Gaussian test problem with $\alpha = 0.5$ and $\beta = 1.5$ using the vw3c scheme with $N = 1000$.

4.3. **Travelling wave.** Glassey et al. [17] discuss weak travelling wave solutions

$$\psi(x,t) = \psi(x - st)$$

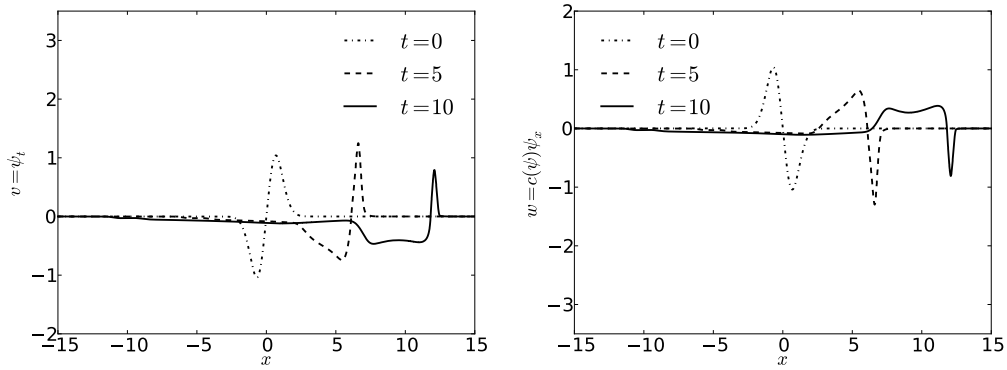

(A) v (B) w

FIGURE 4.4. The numerical solution of the Gaussian test problem with $\alpha = 0.5$ and $\beta = 1.5$ using the vw3d scheme with $N = 1000$.

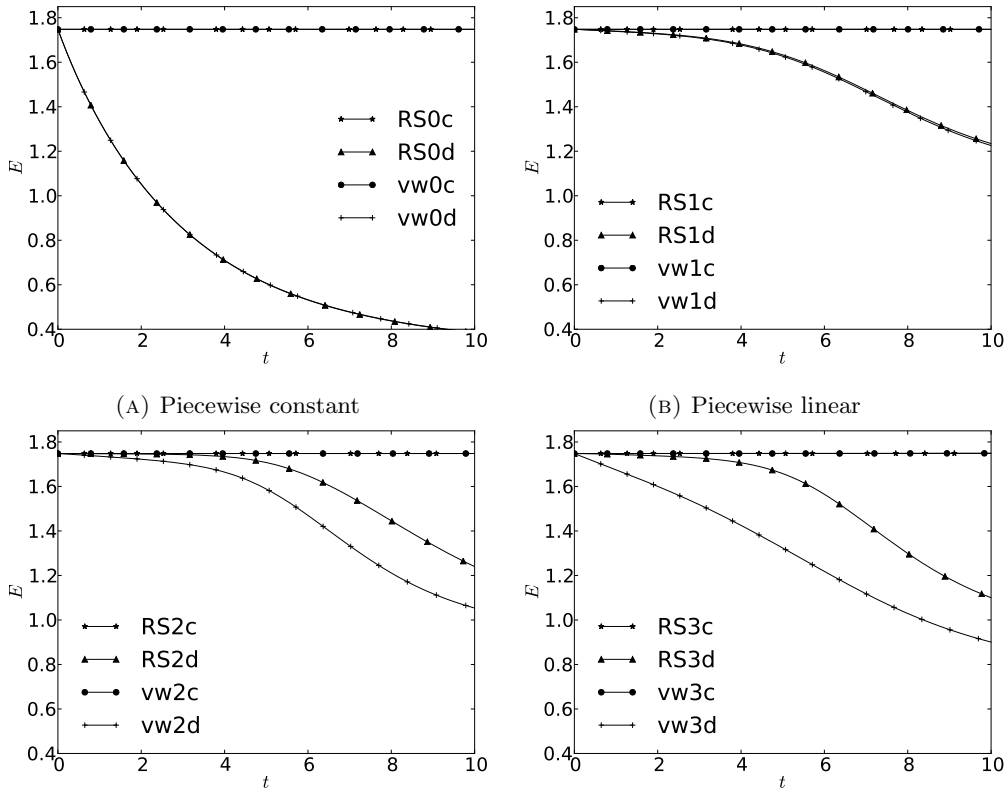

(A) Piecewise constant (B) Piecewise linear

(C) Piecewise quadratic (D) Piecewise cubic

FIGURE 4.5. Evolution of the discrete energy (4.8) and (4.9) for the numerical solution of the Gaussian test problem with $\alpha = 0.5$ and $\beta = 1.5$ using $N = 1000$.

for the non-linear variational wave equation. Such a solution must fulfil

$$\psi' \sqrt{|s^2 - \alpha \cos^2(\psi) - \beta \sin^2(\psi)|} = k, \tag{4.10}$$

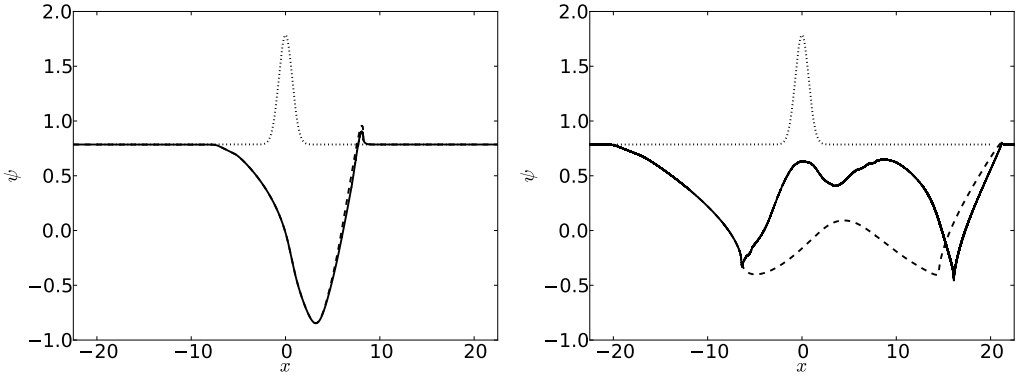

(A) $t = 4$ (B) $t = 12$

FIGURE 4.6. The numerical solution of the Gaussian test problem with $\alpha = 0.5$ and $\beta = 4.5$ using the conservative vw3c (solid) and dissipative vw3d (dashed) schemes using $N = 10000$. The dotted line is the Gaussian initial data.

TABLE 4.4. The error $\|\psi - \psi_{\text{ref}}\|_2$ for the conservative vw schemes at $t = 12$ for the Gaussian initial with $\alpha = 0.5$ and $\beta = 4.5$ with $N = 20 \times 2^i$. The reference solution was computed using the vw3c scheme with $N = 10000$.

i	3	4	5	6	7
vw0c	2.8578	4.5302	4.2199	3.5382	3.0693
vw1c	4.9764	4.3353	3.5673	3.0770	2.8096
vw2c	2.3927	1.3466	1.2581	1.1201	1.0295
vw3c	1.1941	0.7812	0.5205	0.3233	0.1284

TABLE 4.5. The error $\|\psi - \psi_{\text{ref}}\|_2$ for the dissipative vw schemes at $t = 12$ for the Gaussian initial with $\alpha = 0.5$ and $\beta = 4.5$ with $N = 20 \times 2^i$. The reference solution was computed using the vw3d scheme with $N = 10000$.

i	3	4	5	6	7
vw0d	2.1145	2.5536	2.3978	1.9990	1.5677
vw1d	1.7964	1.8323	1.3663	0.8331	0.4608
vw2d	1.5586	1.2176	0.8640	0.4668	0.2050
vw3d	0.6370	0.3370	0.1764	0.0897	0.0417

where k is some integration constant. By choosing $s = \alpha^{1/2}$ we can write

$$\psi' \sin(\psi) = \frac{k}{|\alpha - \beta|^{1/2}}. \tag{4.11}$$

Then by integrating (4.11) with boundary conditions $\psi(0) = 0$ and $\psi(1) = \pi$, we obtain a travelling-wave solution given explicitly as

$$\psi(x,t) = \begin{cases} 0 & x \le \sqrt{\alpha}t \\ \cos^{-1}\left(-2(x - \sqrt{\alpha}t) + 1\right) & \sqrt{\alpha}t < x < 1 + \sqrt{\alpha}t \\ \pi & x \ge 1 + \sqrt{\alpha}t \end{cases} \tag{4.12}$$

with

$$\psi_x(x,t) = \begin{cases} 0 & x \leq \sqrt{\alpha}t \\ \frac{1}{\sqrt{x-x^2}} & \sqrt{\alpha}t < x < 1+\sqrt{\alpha}t \\ 0 & x \geq 1+\sqrt{\alpha}t \end{cases}. \tag{4.13}$$

We numerically solve the initial value problem given by the nonlinear variational wave equation and the initial data (4.12)–(4.13) with $\alpha = 0.5$ and $\beta = 1.5$. Figure 4.7 and Figure 4.8 show the numerical solution at $t = 1$ with $N = 1000$ using the conservative and dissipative RS schemes, respectively. Results for the vw schemes are similar, and are omitted here to avoid unnecessary redundancy. The numerical solutions are consistent with those reported by Koley et al. [22]. We observe that the strong singularities at the break points cause some numerical irregularities, but overall the schemes are able to capture the travelling wave and become more accurate for higher polynomial order p.

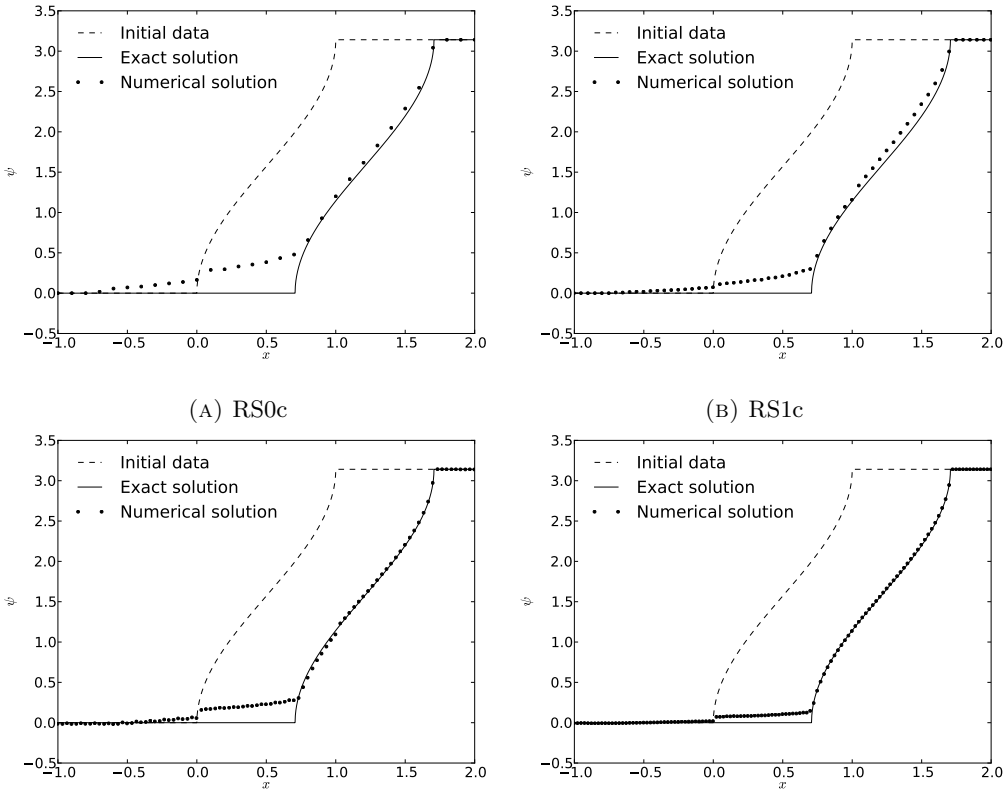

(A) RS0c (B) RS1c

(C) RS2c (D) RS3c

FIGURE 4.7. Numerical solution of the travelling wave initial-value problem with $\alpha = 0.5$ and $\beta = 1.5$ at $t = 1$ using the conservative schemes based on the RS formulation with $N = 1000$.

5. Conclusion

We have considered a nonlinear variational wave equation that models one-dimensional planar waves in nematic liquid crystals. The variational wave equation (1.3) was written in the form of two equivalent first-order systems. An intrinsic property of this equation is the formation of singularities in finite time and the existence of both conservative and dissipative weak solutions. We have constructed robust discontinuous Galerkin schemes for approximating the variational wave equation in one space dimension. The key design principle was energy conservation (dissipation),

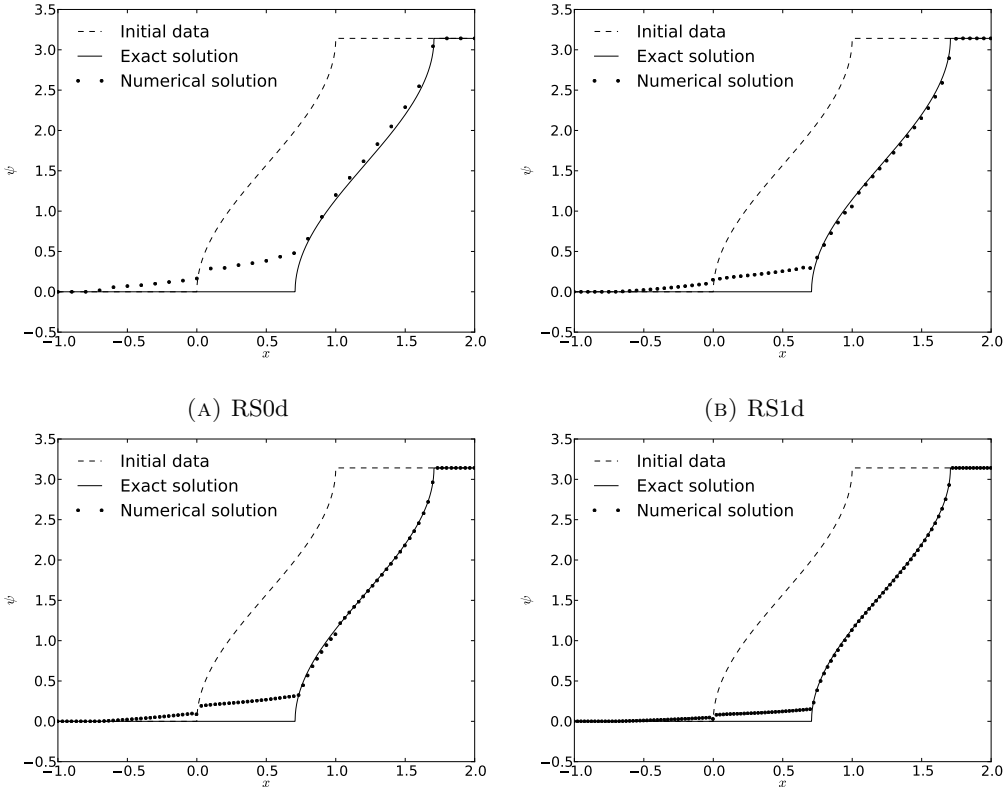

(A) RS0d (B) RS1d

(C) RS2d (D) RS3d

FIGURE 4.8. Numerical solution of the travelling wave initial-value problem with $\alpha = 0.5$ and $\beta = 1.5$ at $t = 1$ using the dissipative schemes based on the RS formulation with $N = 1000$.

and we have designed high-order semi-discrete schemes that either conserve or dissipate the discrete energy.

Extensive numerical experiments have been presented to illustrate the properties of the DG schemes. The high-order accuracy of the methods was demonstrated using a manufactured smooth solution. It has been shown numerically that the energy conservative and energy dissipative schemes converge to two different solutions when the mesh is refined. To the best of our knowledge, these are the first high-order accurate schemes that can approximate the conservative solutions of the one-dimensional variational wave equation.

There exists a generalization to the current model for 2D. Similar numerical schemes can be developed in this case. Herein, the vw formulation must be used since the Riemann invariants are not defined. This will be the topic of an upcoming paper.

APPENDIX A. GLL POINTS, LAGRANGIAN INTERPOLANTS AND DERIVATIVE MATRICES

A.1. **Piecewise constant** ($p = 0$)**.** For the piecewise constant case the single GLL point is $\xi_0 = 0$ with quadrature weight $\rho_0 = 2$. The derivative matrix is in this case simply given by $D = 0$.

A.2. **Piecewise linear** ($p = 1$)**.** In this case the two GLL points are $\xi_0 = -1$, $\xi_1 = 1$, the weights are $\rho_0 = \rho_1 = 1$.

The Lagrangian interpolants are then given explicitly by

$$\ell_0(\xi) = \frac{1-\xi}{2}, \quad \ell_1(\xi) = \frac{1+\xi}{2}, \tag{A.1}$$

and the derivative matrix is

$$D = \begin{pmatrix} -\frac{1}{2} & \frac{1}{2} \\ -\frac{1}{2} & \frac{1}{2} \end{pmatrix}.$$

A.3. **Piecewise quadratic** ($p = 2$)**.** In the piecewise quadratic case the GLL points are $\xi_0 = -1$, $\xi_1 = 0$ and $\xi_2 = 1$ and the weights are $\rho_0 = 1/3$, $\rho_1 = 4/3$ and $\rho_2 = 1/3$.

The Lagrangian interpolants are then given explicitly by

$$\ell_0(\xi) = \frac{1}{2}\xi(\xi - 1), \quad \ell_1(\xi) = 1 - \xi^2, \quad \ell_2(\xi) = \frac{1}{2}\xi(\xi + 1). \tag{A.2}$$

The derivative matrix then becomes

$$D = \begin{pmatrix} -\frac{3}{2} & 2 & -\frac{1}{2} \\ -\frac{1}{2} & 0 & \frac{1}{2} \\ \frac{1}{2} & -2 & \frac{3}{2} \end{pmatrix}. \tag{A.3}$$

A.4. **Piecewise cubic** ($p = 3$)**.** For a piecewise cubic scheme we use the GLL points $\xi_0 = -1$, $\xi_1 = -\sqrt{1/5}$, $\xi_2 = \sqrt{1/5}$ and $\xi_3 = 1$. The quadrature weights are given by $\rho_0 = \rho_3 = 1/6$ and $\rho_1 = \rho_2 = 5/6$.

The Lagrangian interpolants are given explicitly as

$$\ell_0(\xi) = -\frac{5}{8}(x - 1)\left(x^2 - \frac{1}{5}\right) = -\frac{5}{8}\left(x^3 - x^2 - \frac{1}{5}x + \frac{1}{5}\right), \tag{A.4}$$

$$\ell_1(\xi) = \frac{5}{8}\sqrt{5}\left(x^2 - 1\right)\left(x - \sqrt{\frac{1}{5}}\right) = \frac{5}{8}\sqrt{5}\left(x^3 - \sqrt{\frac{1}{5}}x^2 - x + \sqrt{\frac{1}{5}}\right), \tag{A.5}$$

$$\ell_2(\xi) = -\frac{5}{8}\sqrt{5}\left(x^2 - 1\right)\left(x + \sqrt{\frac{1}{5}}\right) = -\frac{5}{8}\sqrt{5}\left(x^3 + \sqrt{\frac{1}{5}}x^2 - x - \sqrt{\frac{1}{5}}\right), \tag{A.6}$$

$$\ell_3(\xi) = \frac{5}{8}(x + 1)\left(x^2 - \frac{1}{5}\right) = \frac{5}{8}\left(x^3 + x^2 - \frac{1}{5}x - \frac{1}{5}\right), \tag{A.7}$$

which gives the derivative matrix

$$D = \begin{pmatrix} -3 & \frac{10}{8}\sqrt{5}\left(1 + \sqrt{\frac{1}{5}}\right) & -\frac{10}{8}\sqrt{5}\left(1 - \sqrt{\frac{1}{5}}\right) & -\frac{1}{2} \\ -\frac{10}{8}\left(\frac{1}{5} + \sqrt{\frac{1}{5}}\right) & 0 & \frac{4}{8}\sqrt{5} & \frac{10}{8}\left(\frac{1}{5} - \sqrt{\frac{1}{5}}\right) \\ -\frac{10}{8}\left(\frac{1}{5} - \sqrt{\frac{1}{5}}\right) & -\frac{4}{8}\sqrt{5} & 0 & -\frac{10}{8}\left(\frac{1}{5} + \sqrt{\frac{1}{5}}\right) \\ 0.5 & \frac{10}{8}\sqrt{5}\left(1 - \sqrt{\frac{1}{5}}\right) & \frac{10}{8}\sqrt{5}\left(1 + \sqrt{\frac{1}{5}}\right) & 3 \end{pmatrix}. \tag{A.8}$$

Acknowledgements

The work of Peder Aursand has been funded by the Research Council of Norway (project number 213638). Ujjwal Koley has been supported by a Humboldt Research Fellowship through the Alexander von Humboldt Foundation.

We are grateful to Professor Siddhartha Mishra for his help and advice in the development of these numerical schemes. The authors would also like to thank Professor Nils Henrik Risebro and Professor Helge Holden for fruitful advice in the course of the preparation of this manuscript.

References

[1] S. Badia, F. Guillén. González and J. V. Gutiérrez–Santacreu. An overview on Numerical Analyses of Nematic Liquid Crystal flows, *Arch. Comput. Methods Eng.*, 18: 285–313 (2011).

[2] S. Badia, F. Guillén. González and J. V. Gutiérrez–Santacreu. Finite element approximation of nematic liquid crystal flows using a saddle-point structure, *J. Comput. Phys.*, 230(4): 1686–1706 (2011).

[3] S. Bartels and A. Prohl. Constraint preserving implicit finite element discretization of harmonic map heat flow into spheres, *Math. Comput.*, 76: 1847–1859 (2007).

[4] T. J. Barth. Numerical methods for gas-dynamics systems on unstructured meshes. In: *An introduction to recent developments in theory and numerics of conservation laws Lecture notes in computational science and engineering*, vol(5), Springer, Berlin. Eds: D Kroner, M. Ohlberger, and C. Rohde, 1999.

[5] R. Becker, X. Feng and A. Prohl. Finite element approximations of the Ericksen–Leslie model for nematic liquid crystal flow, *SIAM J. Numer. Anal.*, 46(4): 1704–1731 (2008).

[6] H. Berestycki, J. M. Coron and I. Ekeland. Variational Methods, Progress in nonlinear differential equations and their applications, *Vol 4*, Birkhäuser, Boston, 1990.

[7] A. Bressan and Y. Zheng. Conservative solutions to a nonlinear variational wave equation, *Commun. Math. Phys.*, 266: 471–497 (2006).

[8] G. Chavent and B. Cockburn. The local projection p^0p^1-discontinuous Galerkin finite element methods for scalar conservation law, *Math. Model. Numer. Anal.*, 23: 565–592 (1989).

[9] D. Christodoulou and A. Tahvildar-Zadeh. On the regularity of Spherically symmetric wave maps, *Comm. Pure Appl. Math.*, 46: 1041–1091 (1993).

[10] S. Y. Cockburn, B. Lin and C. W. Shu. TVB Runge-Kutta local projection discontinuous Galerkin finite element methods for conservation laws III: one dimensional systems, *J. Comput. Phys.*, 84: 90–113 (1989).

[11] J. Coron, J. Ghidaglia and F. Hélein. *Nematics*, Kluwer Academic Publishers, Dordrecht, 1991.

[12] R. J. Diperna and A. Majda. Oscillations and Concentrations in weak solutions of the incompressible fluid equations, *Comm. Math. Phys*, 108: 667–689 (1987).

[13] J. L. Ericksen and D. Kinderlehrer. Theory and application of Liquid Crystals, *IMA Volumes in Mathematics and its Applications*, Vol 5, Springer Verlag, New York, 1987.

[14] R. T. Glassey. Finite-time blow-up for solutions of nonlinear wave equations, *Math. Z.*, 177: 1761–1794 (1981).

[15] S. Gottlieb, C.-W. Shu and E. Tadmor. Strong stability preserving high-order time discretization methods, *SIAM Review*, 43(1): 89-112 (2001).

[16] R. Glassey, J. Hunter, and Y. Zheng. Singularities and Oscillations in a nonlinear variational wave equation. In: J. Rauch and M. Taylor, editors, *Singularities and Oscillations*, Volume 91 of the IMA volumes in Mathematics and its Applications, pages 37–60. Springer, New York, 1997.

[17] R. T. Glassey, J. K. Hunter and Yuxi. Zheng. Singularities of a variational wave equation, *J. Diff. Eq.*, 129: 49–78 (1996).

[18] T. R. Hill and W. H. Reed. Triangular mesh methods for neutron transport equation, *Tech. Rep. LA-UR-73-479.*, Los Alamos Scientific Laboratory, 1973.

[19] H. Holden and X. Raynaud. Global semigroup for the nonlinear variational wave equation, *Arch. Rat. Mech. Anal.*, 201(3): 871–964 (2011).

[20] H. Holden, K. H. Karlsen, and N. H. Risebro. A convergent finite-difference method for a nonlinear variational wave equation, *IMA. J. Numer. Anal.*, 29(3): 539–572 (2009).

[21] J. K. Hunter and R. A. Saxton. Dynamics of director fields, *SIAM J. Appl. Math.*, 51: 1498–1521 (1991).

[22] U. Koley, S. Mishra, N. H. Risebro, and F. Weber. Robust finite-difference schemes for a nonlinear variational wave equation modeling liquid crystals, *Submitted*.

[23] F. H. Lin and C. Liu. Non-parabolic dissipative systems modelling the flow of liquid crystals, , *Comm. Pure Appl. Math.*, 48, 501–537 (1995).

[24] F. H. Lin and C. Liu. Existence of solutions for the Ericksen-Leslie system, *Arch. Ration. Mech. Anal.*, 154, 135–156 (2000).

[25] H. A. Luther and H. P. Konen. Some fifth-order classical Runge–Kutta formulas *SIAM Review*, 7(4): 551–558 (1965).

[26] R. A. Saxton. Dynamic instability of the liquid crystal director, *Contemporary Mathematics Vol 100*, Current Progress in Hyperbolic Systems, pages 325–330, ed. W. B. Lindquist, AMS, Providence, 1989.

[27] J. Shatah. Weak solutions and development of singularities in the SU(2) σ-model, *Comm. Pure Appl. Math.*, 41: 459–469 (1988).

[28] J. Shatah and A. Tahvildar-Zadeh. Regularity of harmonic maps from Minkowski space into rotationally symmetric manifolds, *Comm. Pure Appl. Math*, 45: 947–971 (1992).

[29] C.-W. Shu. Different formulations of the discontinuous Galerkin method for the viscous terms, In: *Conference in Honor of Professor H.-C. Huang on the occasion of his retirement*, Science Press, 14–45, 2000.

[30] P. Zhang and Y. Zheng. On oscillations of an asymptotic equation of a nonlinear variational wave equation, *Asymptot. Anal.*, 18(3): 307–327 (1998).

[31] P. Zhang and Y. Zheng. Singular and rarefactive solutions to a nonlinear variational wave equation, *Chin. Ann. Math.*, 22: 159–170 (2001).

[32] P. Zhang and Y. Zheng. Rarefactive solutions to a nonlinear variational wave equation of liquid crystals, *Commun. Partial Differ. Equ.*, 26: 381–419 (2001).

[33] P. Zhang and Y. Zheng. Weak solutions to a nonlinear variational wave equation, *Arch. Rat. Mech. Anal.*, 166: 303–319 (2003).
[34] P. Zhang and Y. Zheng. Weak solutions to a nonlinear variational wave equation with general data, *Ann. Inst. H. Poincaré Anal. Non Linéaire*, 22: 207–226 (2005).
[35] P. Zhang and Y. Zheng. On the global weak solutions to a nonlinear variational wave equation, *Handbook of Differential Equations. Evolutionary Equations*, ed. C. M. Dafermos and E. Feireisl, vol. 2, pages 561–648, Elsevier, 2006.

(Peder Aursand)
Department of Mathematical Sciences,
Norwegian University of Science and Technology,
NO–7491 Trondheim, Norway.
E-mail address: peder.aursand@math.ntnu.no

(Ujjwal Koley)
Institut für Mathematik,
Julius-Maximilians-Universität Würzburg,
Campus Hubland Nord, Emil-Fischer-Strasse 30,
97074, Würzburg, Germany.
E-mail address: toujjwal@gmail.com